

Fall 10-1-2012

High-Throughput Synthesis and Analysis for Searching New Permanent Magnet Materials

Gerhard Schneider

Materials Research Institute, Aalen University

Dagmar Goll

Materials Research Institute, Aalen University

Ralf Löffler

Materials Research Institute, Aalen University

Roman Karimi

Follow this and additional works at: http://dc.engconfintl.org/materials_genome



Part of the [Biomedical Engineering and Bioengineering Commons](#)

Recommended Citation

Gerhard Schneider, Dagmar Goll, Ralf Löffler, and Roman Karimi, "High-Throughput Synthesis and Analysis for Searching New Permanent Magnet Materials" in "Harnessing The Materials Genome: Accelerated Materials Development via Computational and Experimental Tools", J.-C. Zhao, The Ohio State Univ.; M. Asta, Univ. of California Berkeley; Peter Gumbsch Institutsleiter Fraunhofer-Institut fuer Werkstoffmechanik IWM; B. Huang, Central South University Eds, ECI Symposium Series, (2013). http://dc.engconfintl.org/materials_genome/6

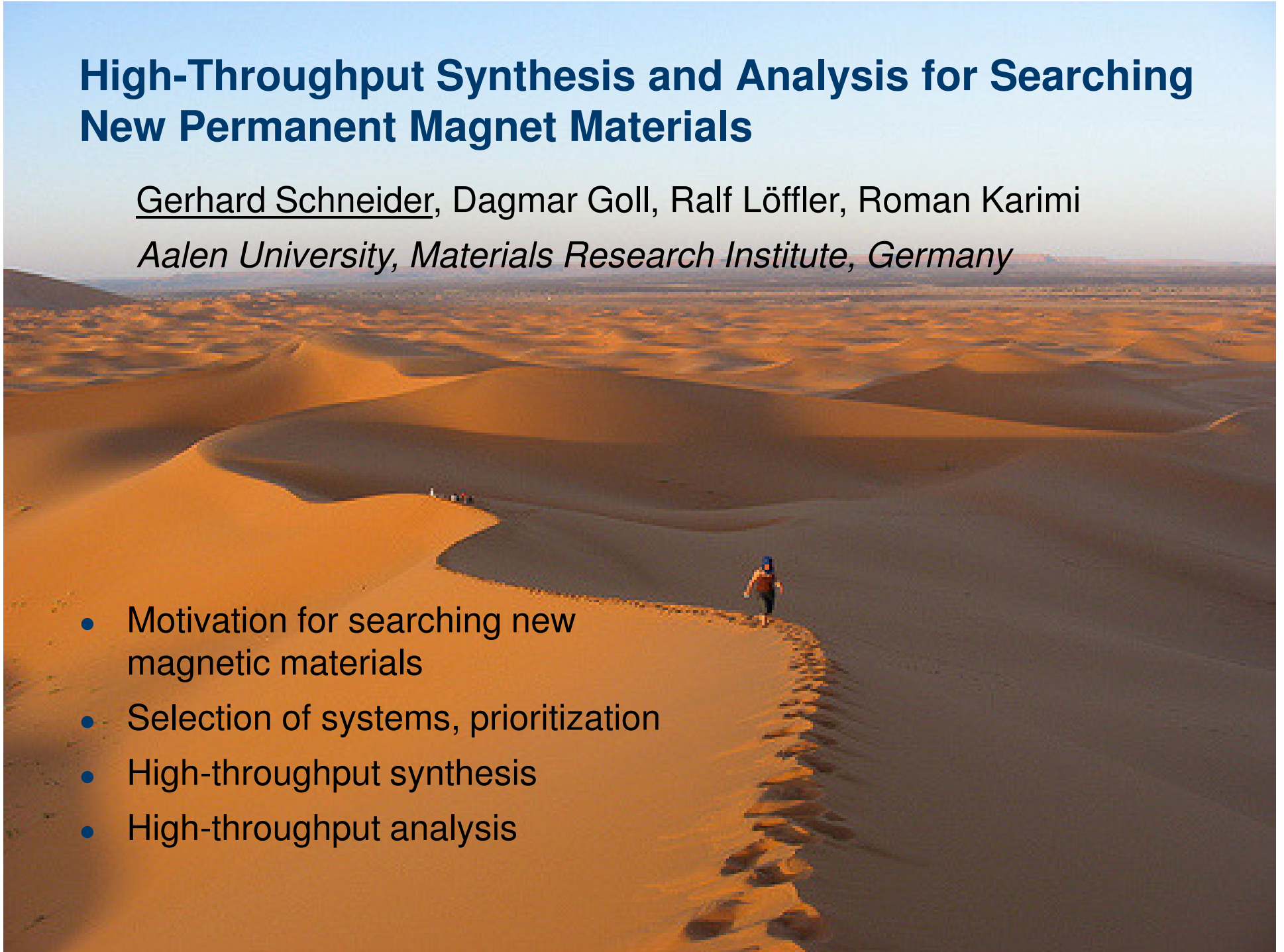
This Conference Proceeding is brought to you for free and open access by the Proceedings at ECI Digital Archives. It has been accepted for inclusion in Harnessing The Materials Genome: Accelerated Materials Development via Computational and Experimental Tools by an authorized administrator of ECI Digital Archives. For more information, please contact franco@bepress.com.

High-Throughput Synthesis and Analysis for Searching New Permanent Magnet Materials

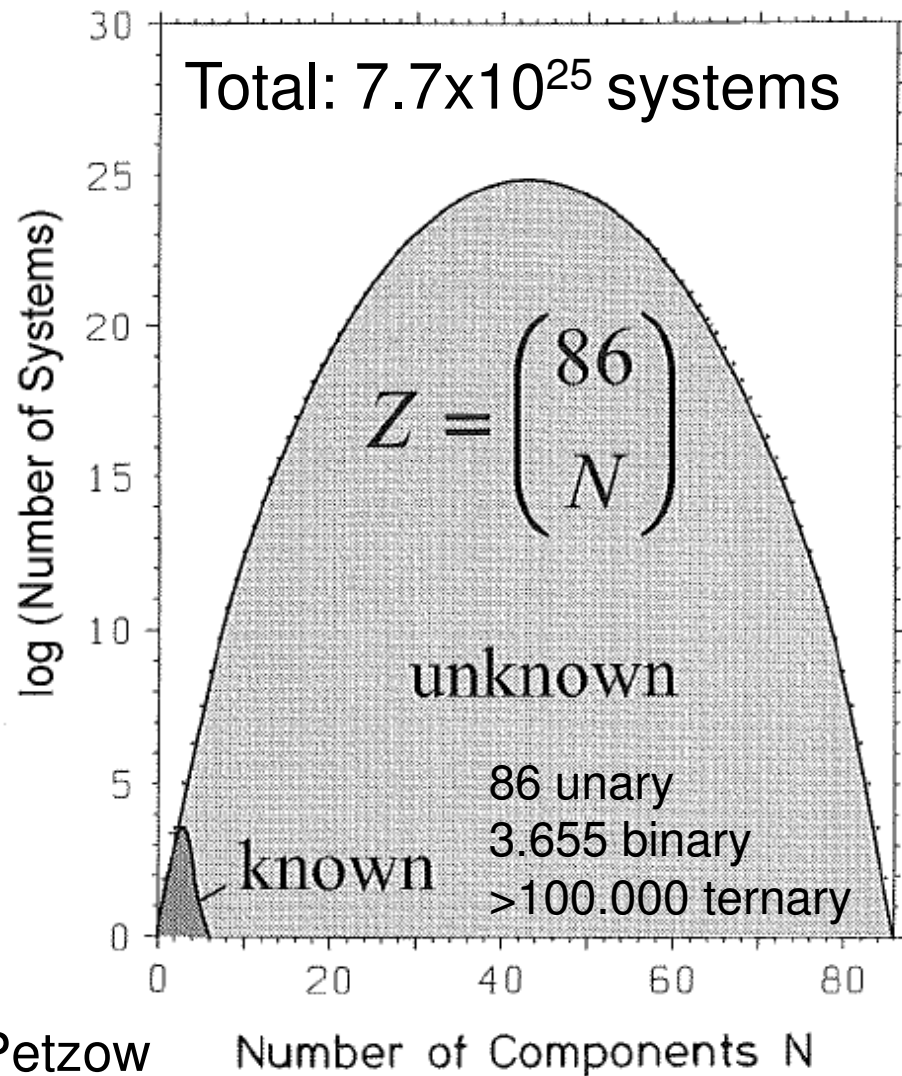
Gerhard Schneider, Dagmar Goll, Ralf Löffler, Roman Karimi

Aalen University, Materials Research Institute, Germany

- Motivation for searching new magnetic materials
- Selection of systems, prioritization
- High-throughput synthesis
- High-throughput analysis



Potential to discover new materials



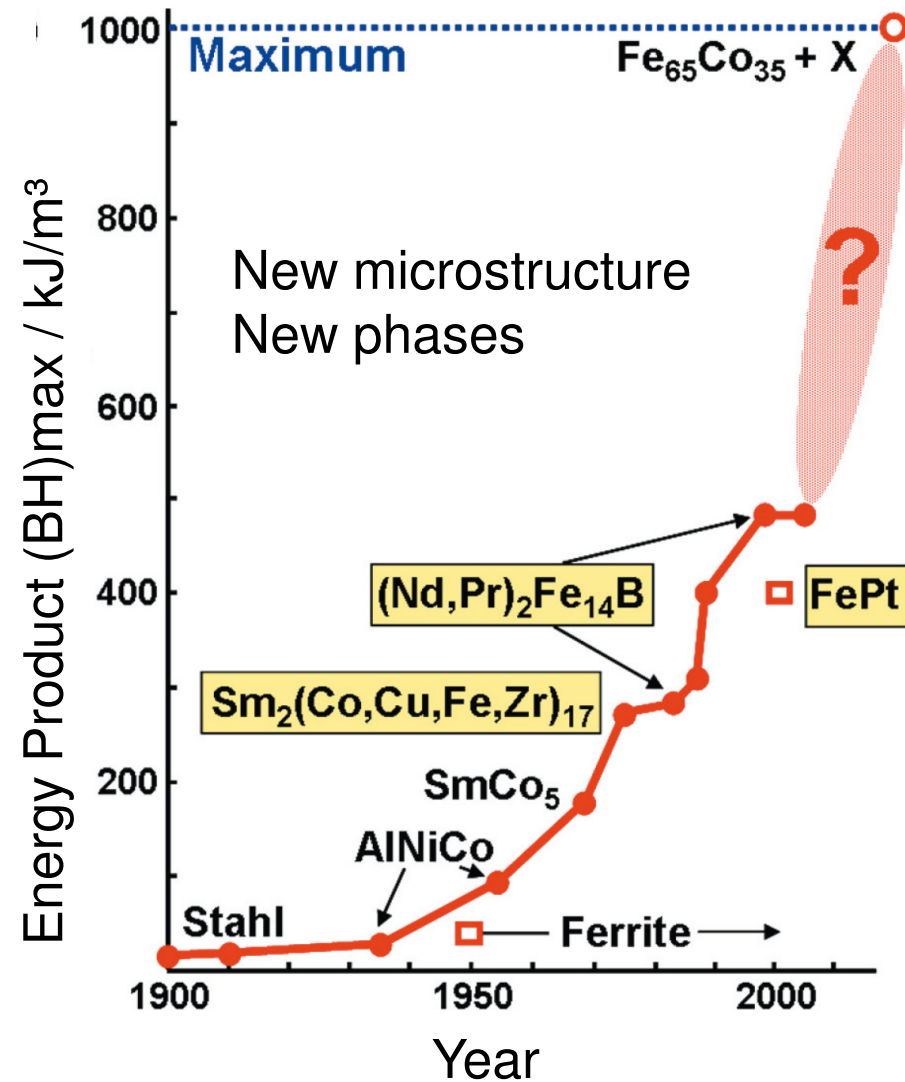
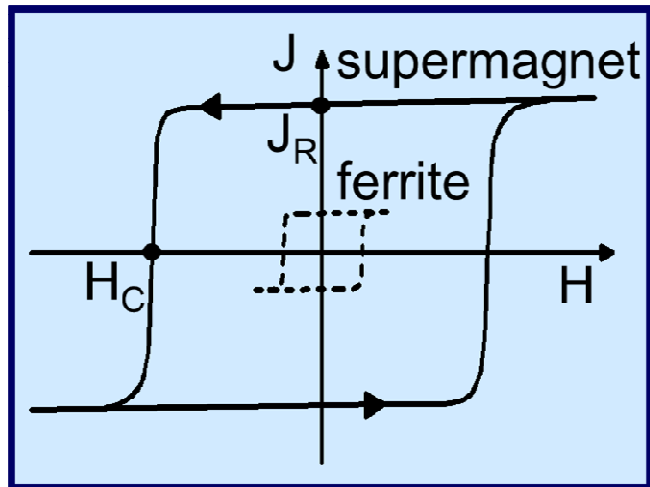
Still great potential to find new materials with specific properties.

Need to develop High-Throughput methods

Motivation for the search of new magnetic phases

Key applications in energy conversion

- Generators
- Motors



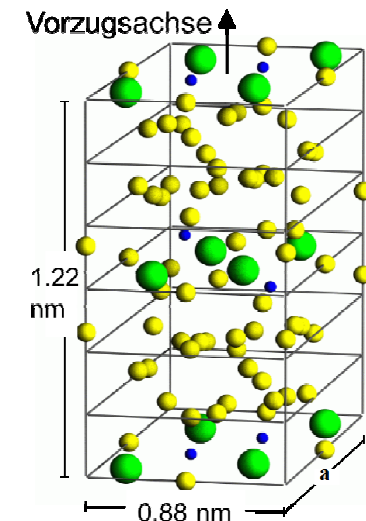
Preconditions for permanent magnets

- Existence/ stability of a phase with excellent intrinsic properties –



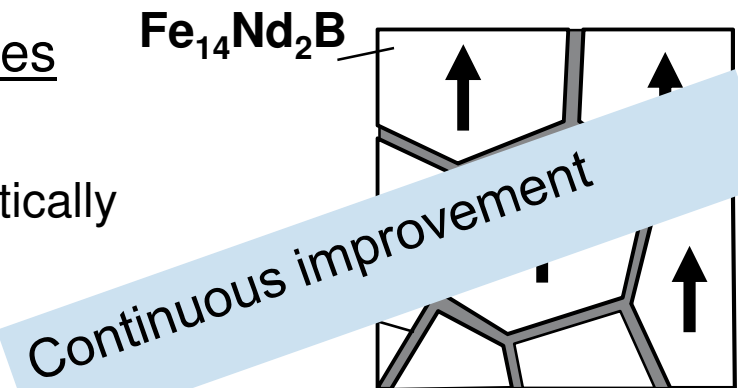
- Magnetocrystalline anisotropy $H_A = 68 \text{ MA/m}$
- Saturation polarization $J_s = 1.63 \text{ T}$
- Curie temperature $T_C = 310 \text{ }^\circ\text{C}$
- ...

disruptive



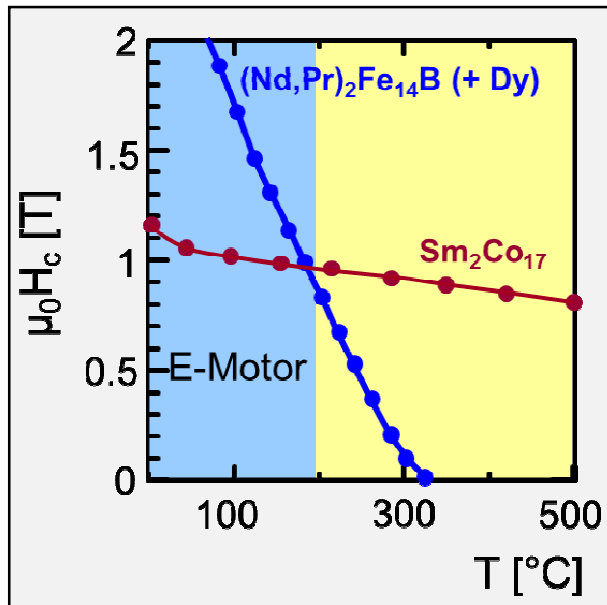
- Microstructure design – extrinsic properties

- Avoid soft magnetic phases
- Isolate aligned single crystal grains magnetically
- Avoid nonmagnetic grains



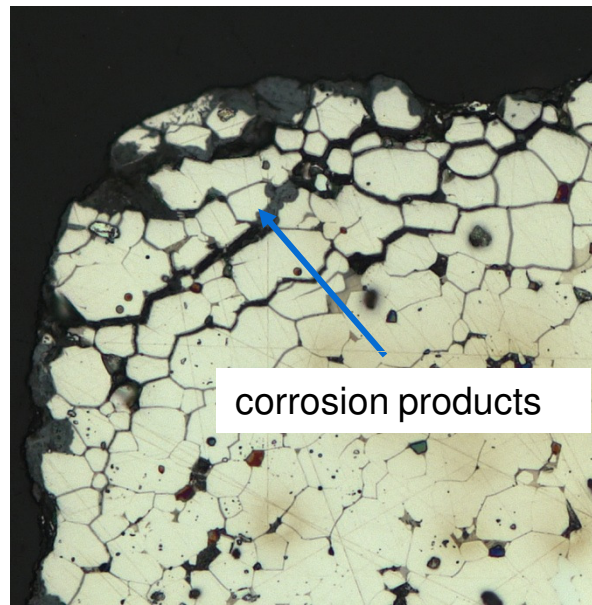
Additional requirements for permanent magnets

Temperature stability



max. operating
Temperature of Fe-Nd-B:
180 °C to 200 °C

Corrosion stability



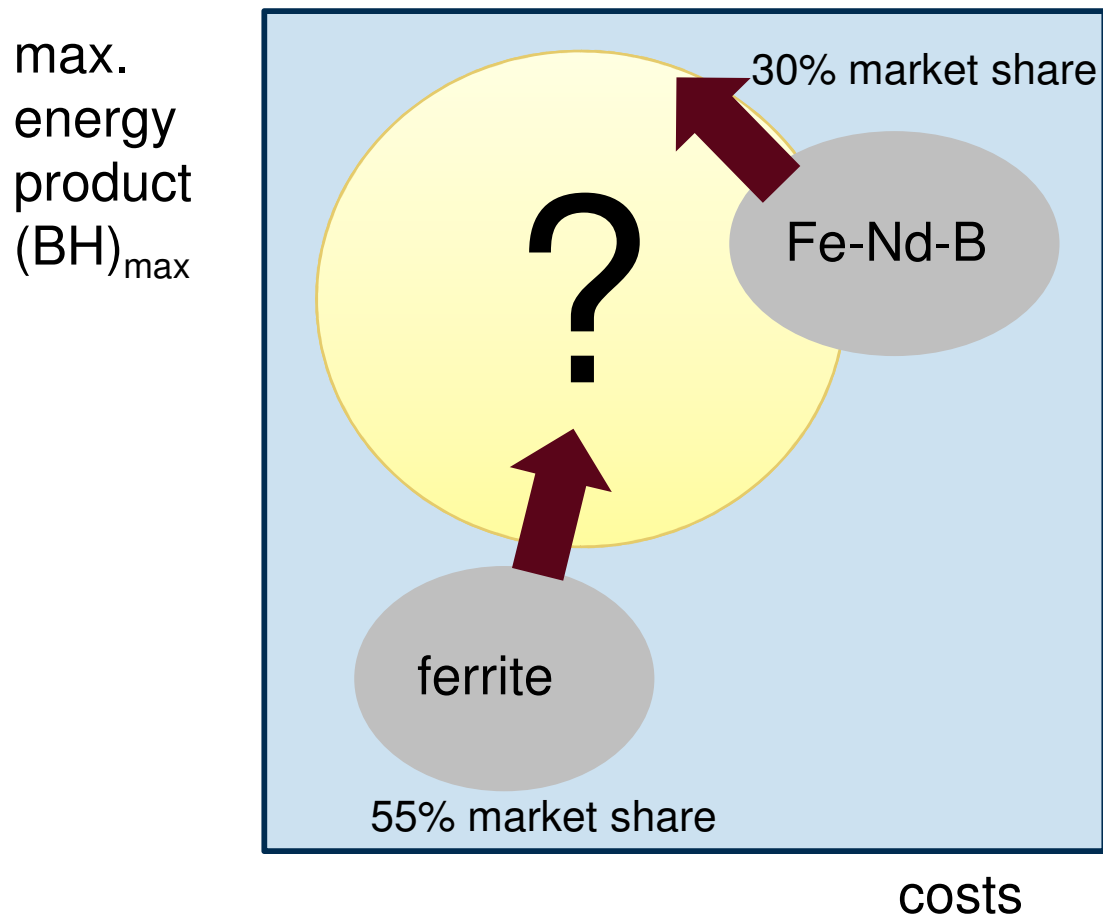
corrosion protection

Raw material aspect



rare earth metals
are expensive
(97 % China)

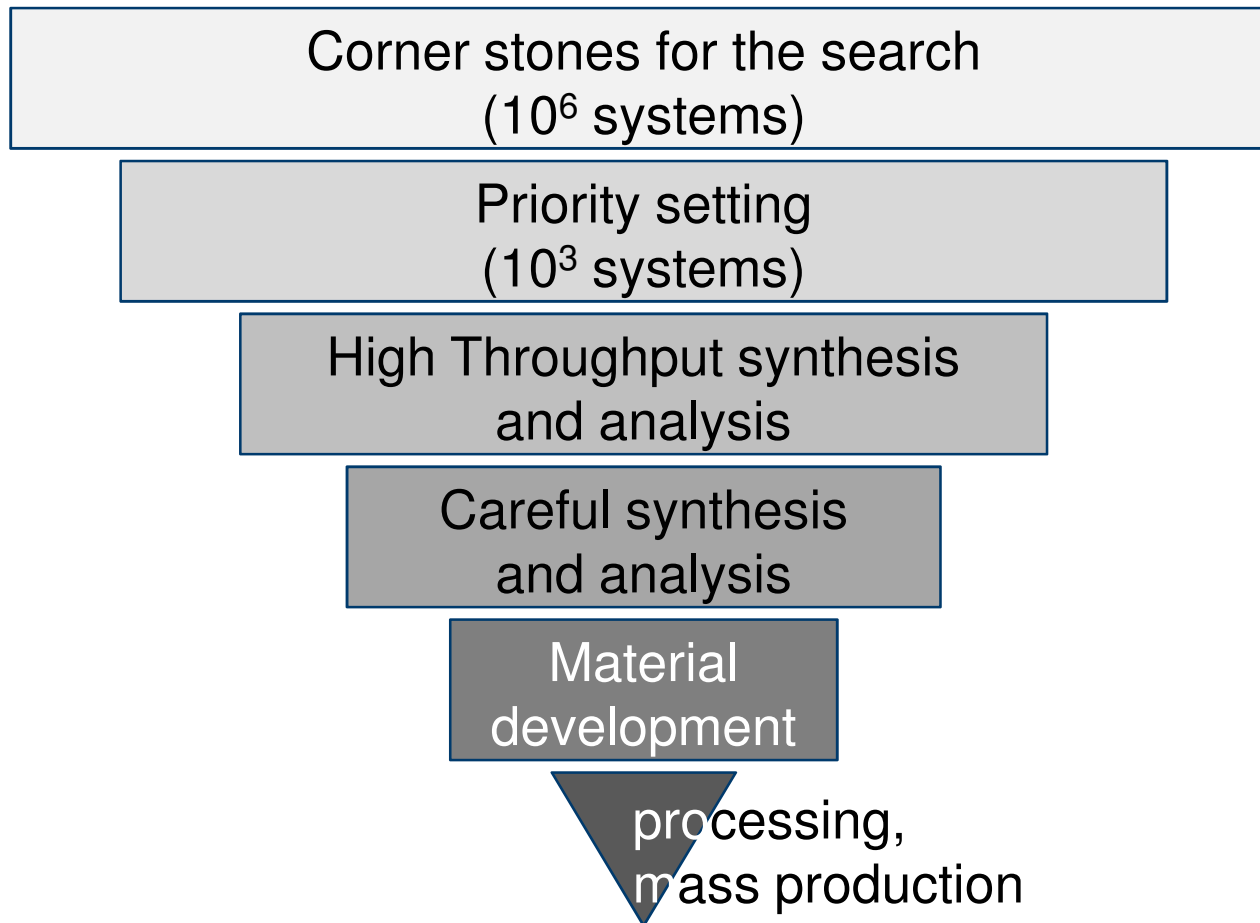
New Permanent Magnet Materials



Development goals:

- Magnetic performance (B_R , H_C , T_C , losses, ...)
- Lower material and processing costs, availability of raw materials
- Durability (aging, corrosion, mechanical properties, ...)

Strategy High-Throughput experimentation



First selection of elements

- Ferromagnetic transition metals (TM)

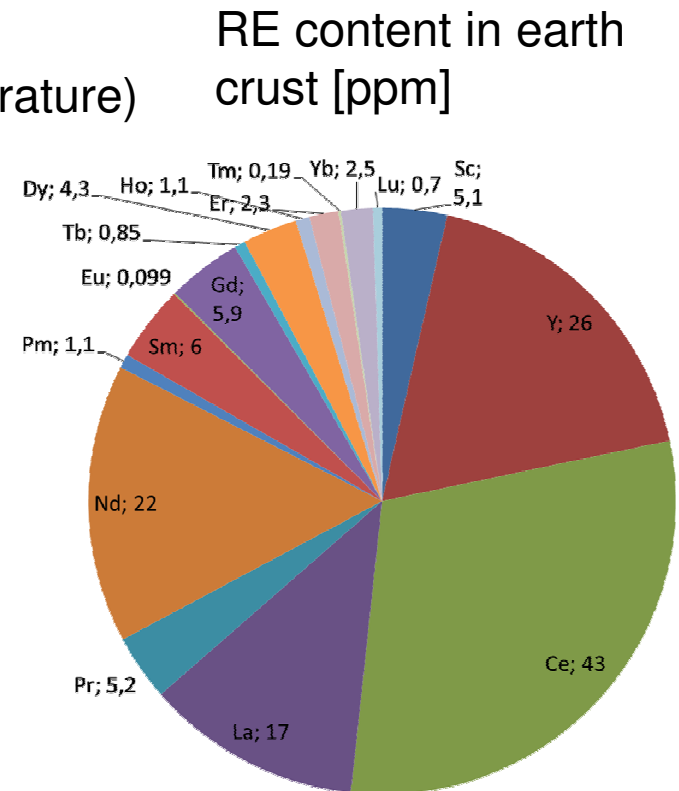
- Basis of ferromagnetism
(high saturation polarization, high Curie temperature)
- Economical

- Rare earth metals (RE)

- Prerequisite for highest anisotropies
- Mischmetals are cheaper than pure RE
- Light RE are cheaper than heavy RE
- La or Ce are available in larger amounts

- Additives

- for stabilization of new phases or improving properties of known phases
- non-toxic, non-radioactive



Estimation of the number of systems

- Selection of elements
 - TM: transition metals: Fe, Co, Ni, Mn; $k = 4$
 - RE: rare earth metals: La, Ce, Y, Pr, Nd, Sm, Dy; $j = 7$
 - Add: additives X; $l = 41$
- RE systems
 - TM (unary), TM-RE (binary), TM-RE-X (ternary)
 - TM1-TM2-RE-X, TM-RE1-RE2-X, TM-RE-X1-X2 (quaternary)

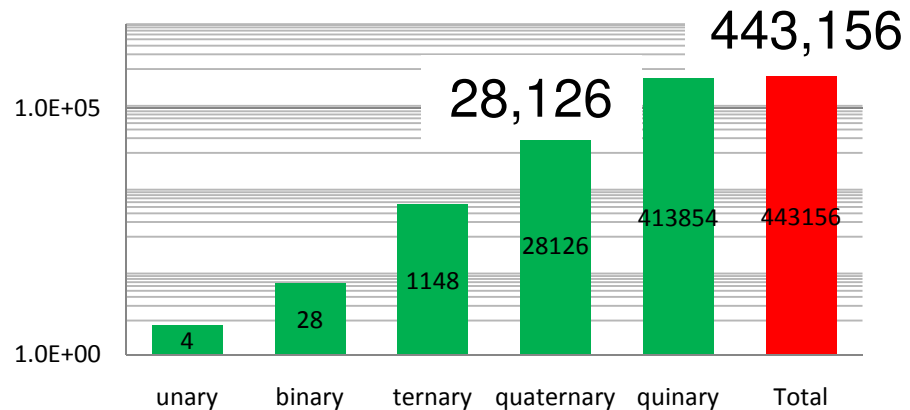
$$\binom{TM}{k} \binom{Add}{l} \binom{RE}{j} = \frac{TM!}{(TM-k)!k!} \frac{Add!}{(Add-l)!l!} \frac{RE!}{(RE-j)!j!}$$

- RE-free systems
 - TM (unary), TM-X (binary), TM1-TM2-X (ternary), TM-X1-X2 (ternary)

$$\binom{TM}{k} \binom{Add}{l} = \frac{TM!}{(TM-k)!k!} \frac{Add!}{(Add-l)!l!}$$

Estimation of the number of interesting systems

RE-containing systems; log 10

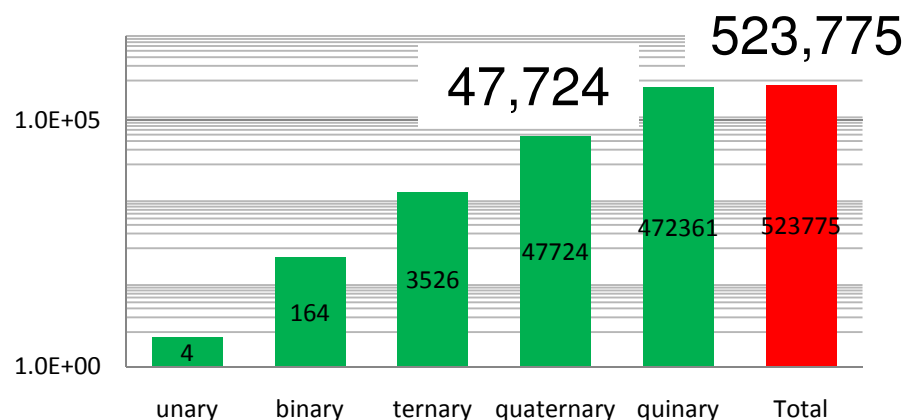


total number of systems: ~ 1.000.000
 known systems: ~ 1000
 ratio: ~ 1:1000

area Northern Ireland
area Europe

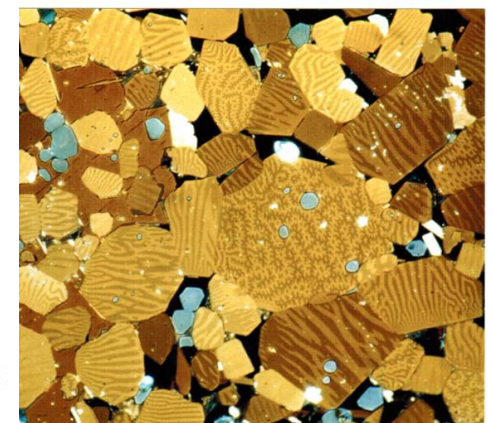
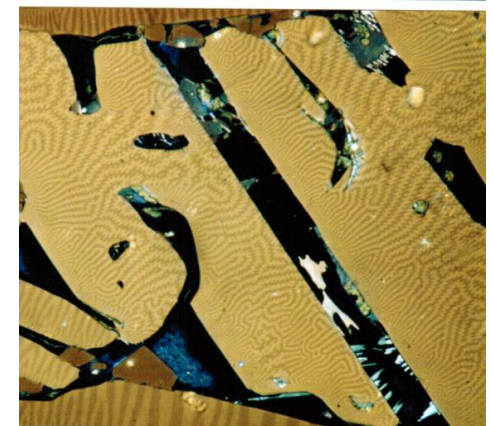
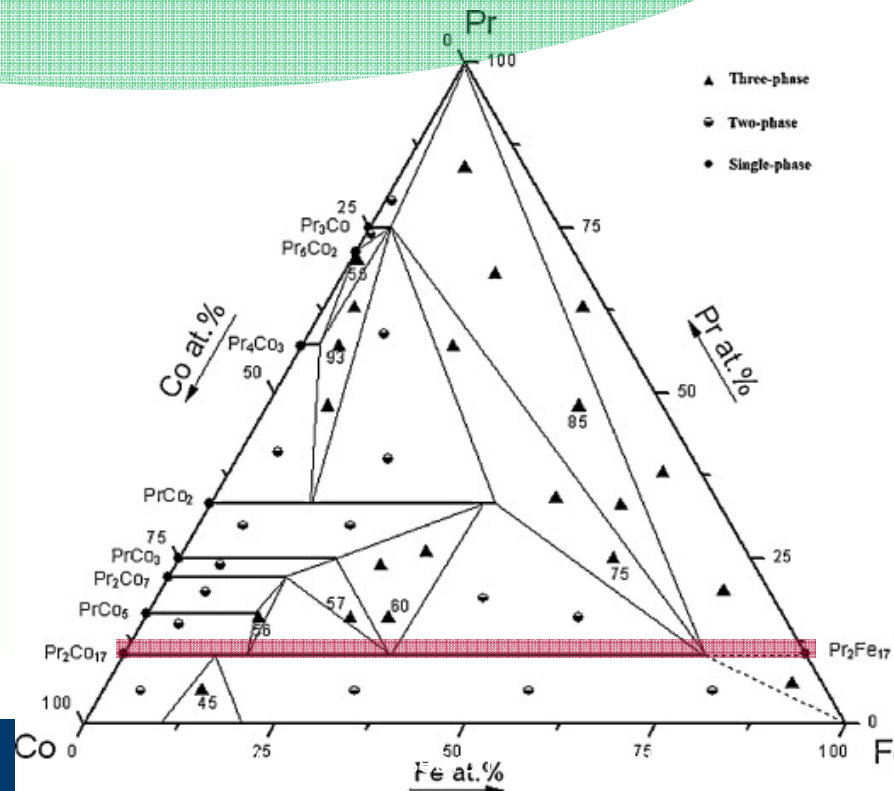
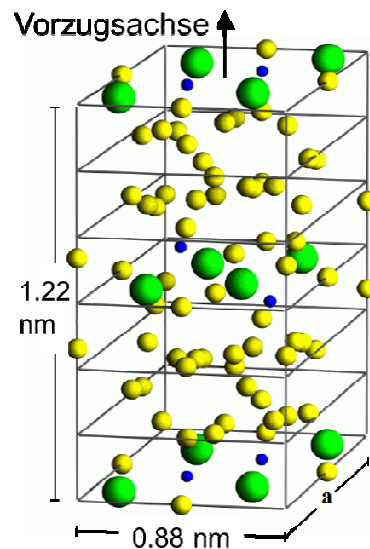


RE-free systems; log 10

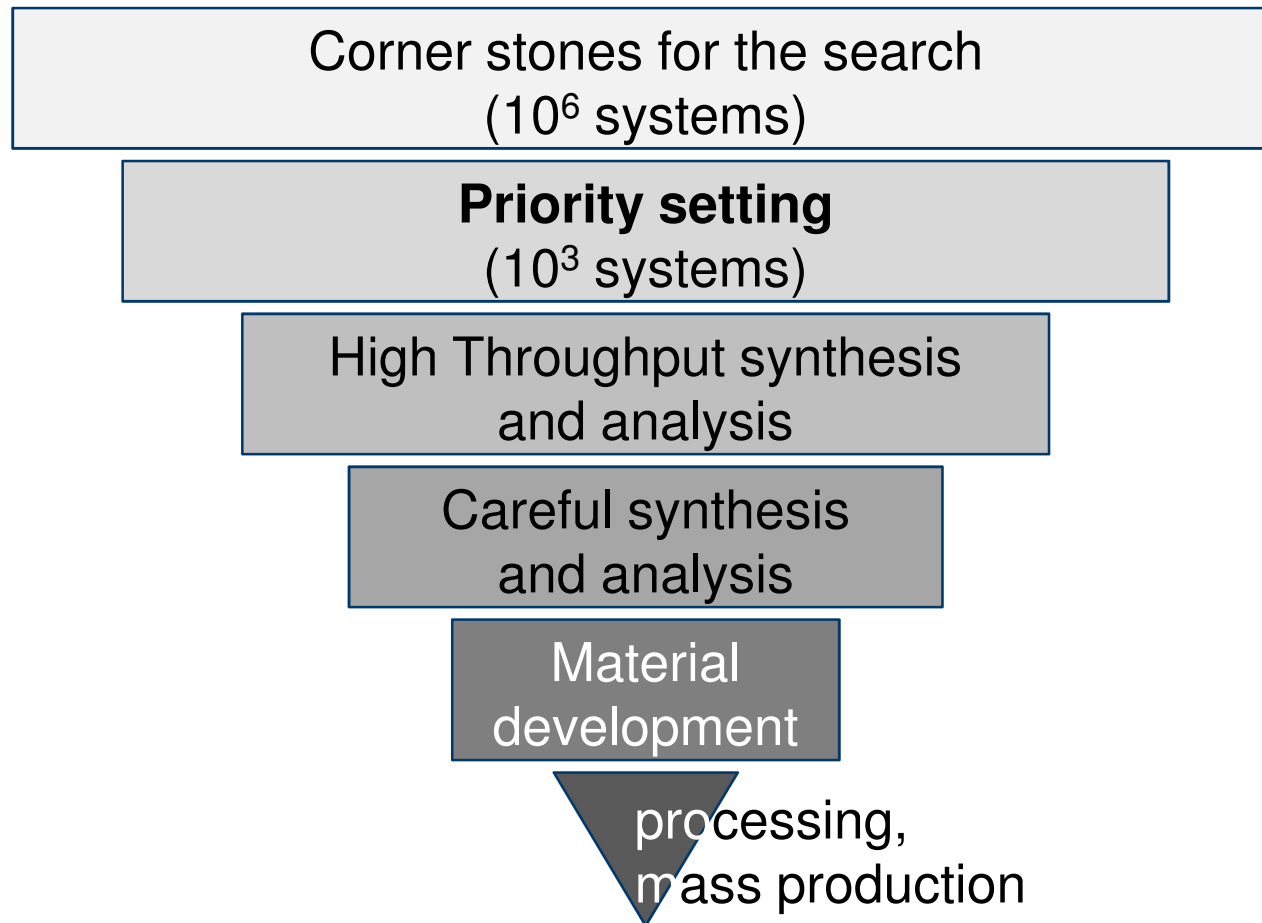


New Phases and modification of known phases

- New Phases
 - New composition
 - New crystal structure
 - Examples:
 - $\text{Fe}_{14}\text{Nd}_2\text{B}$
- Known Phases
 - Homogeneity range
 - Additives
 - Examples:
 - $(\text{Fe},\text{Co})_{17}\text{Pr}_2$
- Microstructure optimization



Strategy High-Throughput experimentation



Prioritization

Input data base

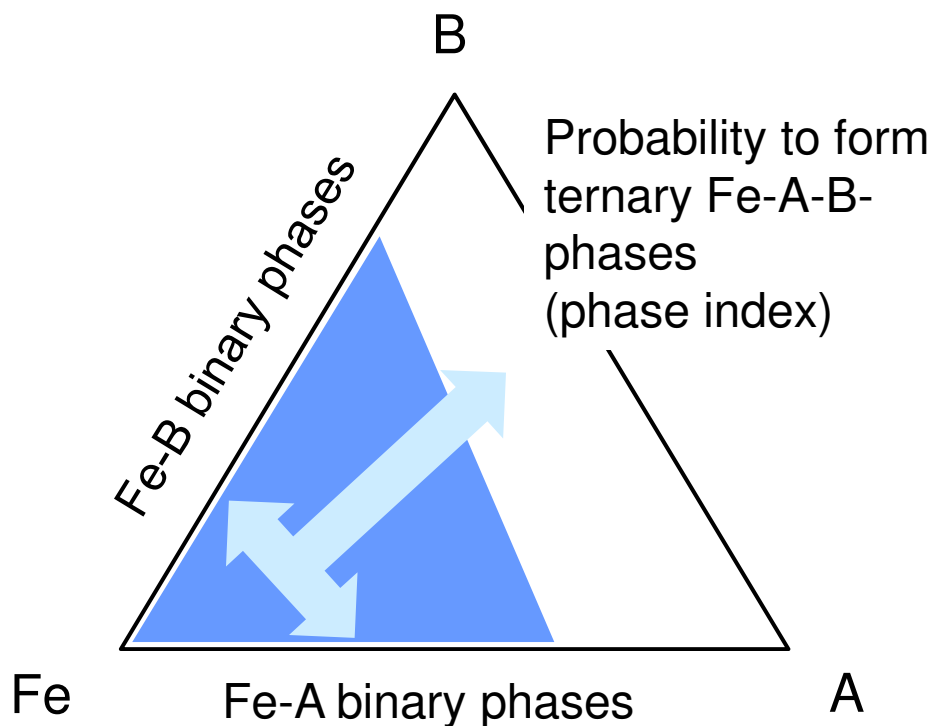
| Fe | Element | Ag | Al | Am | As | Au | B | Ba | Be | Bi | C | Ca | Cd | Ce | Co | Cr | Cs | Cu | Dy | Er | Eu | Ga | Gd | Ge |
|---------|---------------|----|----|----|----|----|----|----|----|----|----|----|----|----|----|----|----|----|----|----|----|----|----|----|
| Element | Anzahl Phasen | 0 | 8 | 1 | 4 | 0 | 3 | 0 | 4 | 0 | 6 | 0 | 0 | 2 | 1 | 1 | 0 | 0 | 4 | 4 | 0 | 5 | 4 | 6 |
| Ag | 0 | x | 0 | 0 | 0 | 0 | 0 | 0 | 0 | 0 | 0 | 0 | 0 | 0 | 0 | 0 | 0 | 0 | 0 | 0 | 0 | 0 | 0 | 0 |
| Al | 8 | 0 | x | 8 | 32 | 0 | 24 | 0 | 32 | 0 | 48 | 0 | 0 | 16 | 8 | 8 | 0 | 0 | 32 | 32 | 0 | 40 | 32 | 48 |
| Am | 1 | 0 | 8 | x | 4 | 0 | 3 | 0 | 4 | 0 | 6 | 0 | 0 | 2 | 1 | 1 | 0 | 0 | 4 | 4 | 0 | 5 | 4 | 6 |
| As | 4 | 0 | 32 | 4 | x | 0 | 12 | 0 | 16 | 0 | 24 | 0 | 0 | 8 | 4 | 4 | 0 | 0 | 16 | 16 | 0 | 20 | 16 | 24 |
| Au | 0 | 0 | 0 | 0 | x | 0 | 0 | 0 | 0 | 0 | 0 | 0 | 0 | 0 | 0 | 0 | 0 | 0 | 0 | 0 | 0 | 0 | 0 | 0 |
| B | 3 | 0 | 24 | 3 | 12 | 0 | x | 0 | 12 | 0 | 18 | 0 | 0 | 6 | 3 | 3 | 0 | 0 | 12 | 12 | 0 | 15 | 12 | 18 |
| Ba | 0 | 0 | 0 | 0 | 0 | 0 | x | 0 | 0 | 0 | 0 | 0 | 0 | 0 | 0 | 0 | 0 | 0 | 0 | 0 | 0 | 0 | 0 | 0 |
| Be | 4 | 0 | 32 | 4 | 16 | 0 | 12 | 0 | x | 0 | 24 | 0 | 0 | 8 | 4 | 4 | 0 | 0 | 16 | 16 | 0 | 20 | 16 | 24 |
| Bi | 0 | 0 | 0 | 0 | 0 | 0 | 0 | 0 | x | 0 | 0 | 0 | 0 | 0 | 0 | 0 | 0 | 0 | 0 | 0 | 0 | 0 | 0 | 0 |
| C | 6 | 0 | 48 | 6 | 24 | 0 | 18 | 0 | 24 | 0 | x | 0 | 0 | 12 | 6 | 6 | 0 | 0 | 24 | 24 | 0 | 30 | 24 | 36 |

List of prioritization

| System | PI * KI |
|--------|---------|
| Fe-Y- | 5 |
| Fe-Sm- | 6 |
| Fe-Ce- | 9 |
| Fe-Y- | 26 |
| Fe-Y- | 28 |
| Fe-Y- | 48 |
| Fe-Sm- | 48 |
| Fe-Y- | 50 |
| Fe-Sm- | 60 |
| Fe-Nd- | 72 |
| Fe-Y- | 72 |

Priority setting (index)

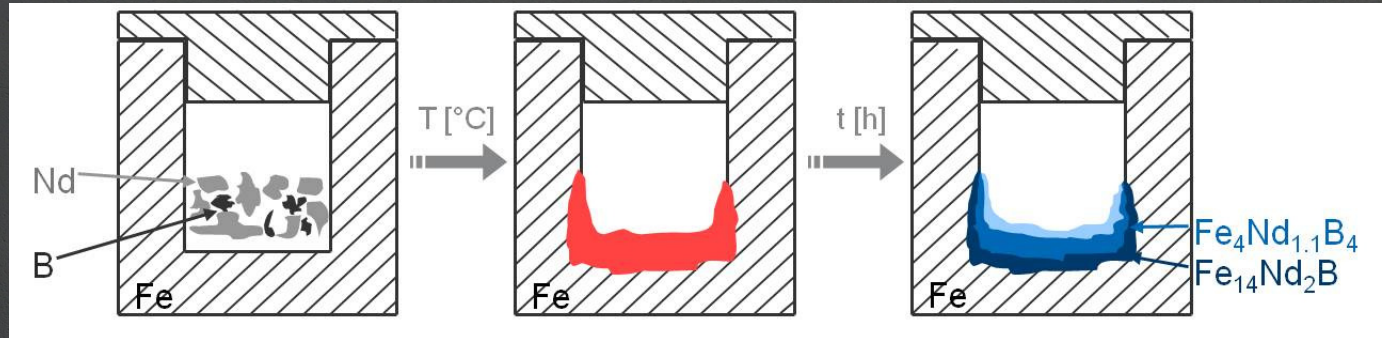
- Non toxic
- Cost efficient/ available
- Probability to form intermediate phases
- Physical principles



Search for new magnetic phases criteria for efficient synthesis

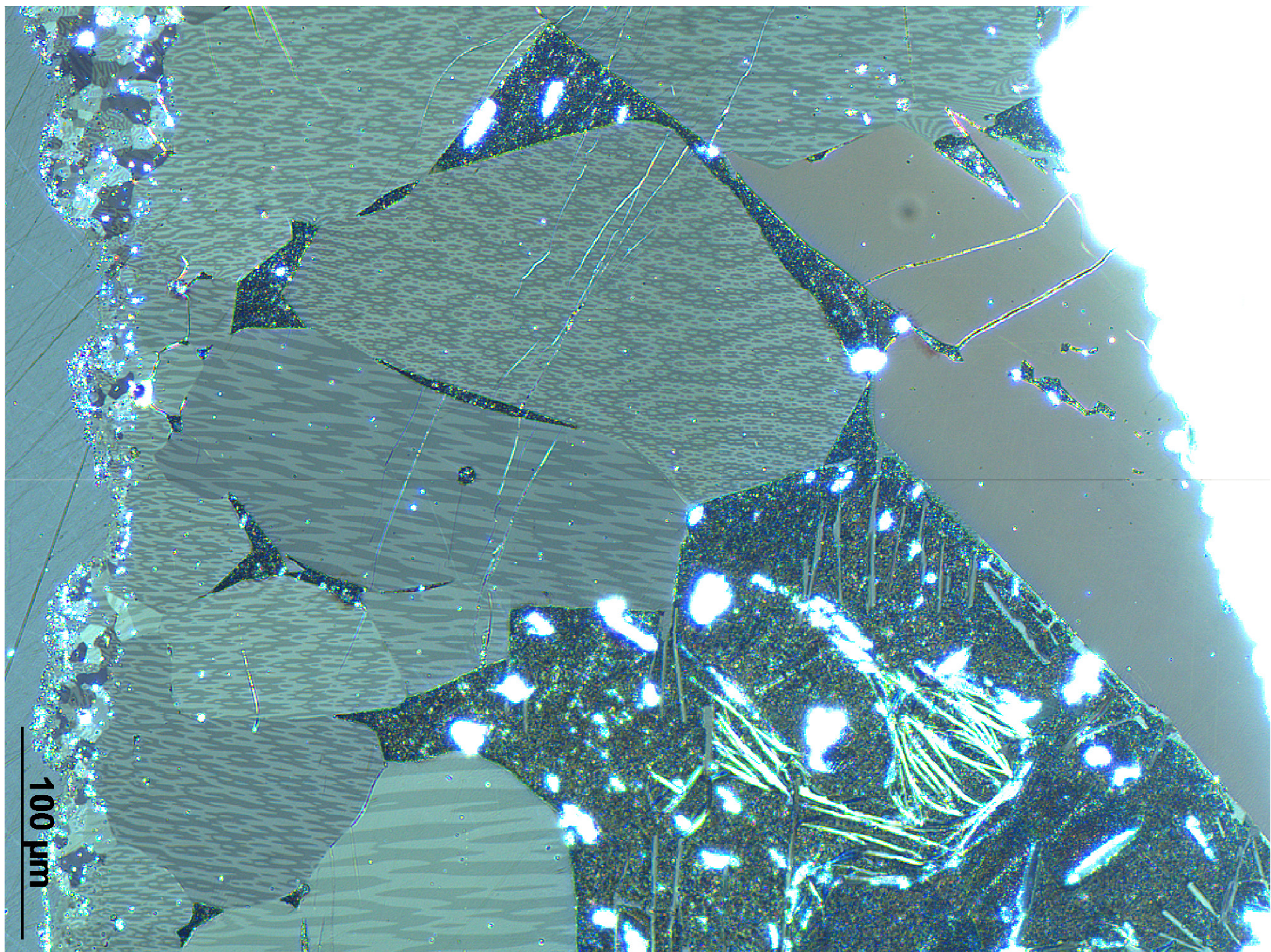
- High probability to receive numerous phases (e.g. stable and metastable)
 - Non-equilibrium states in binary and higher component systems
- Interest focused on TM-rich phases
- Small specimen
- Quick and easy process
- Grain size of new phases should be larger than 10 μm (due to analysis method)

Diffusion Couple Fe-Nd-B



The intermetallic phases form during isothermal annealing and during cooling

2000 μm



Diffusion Couple Fe-Nd-B

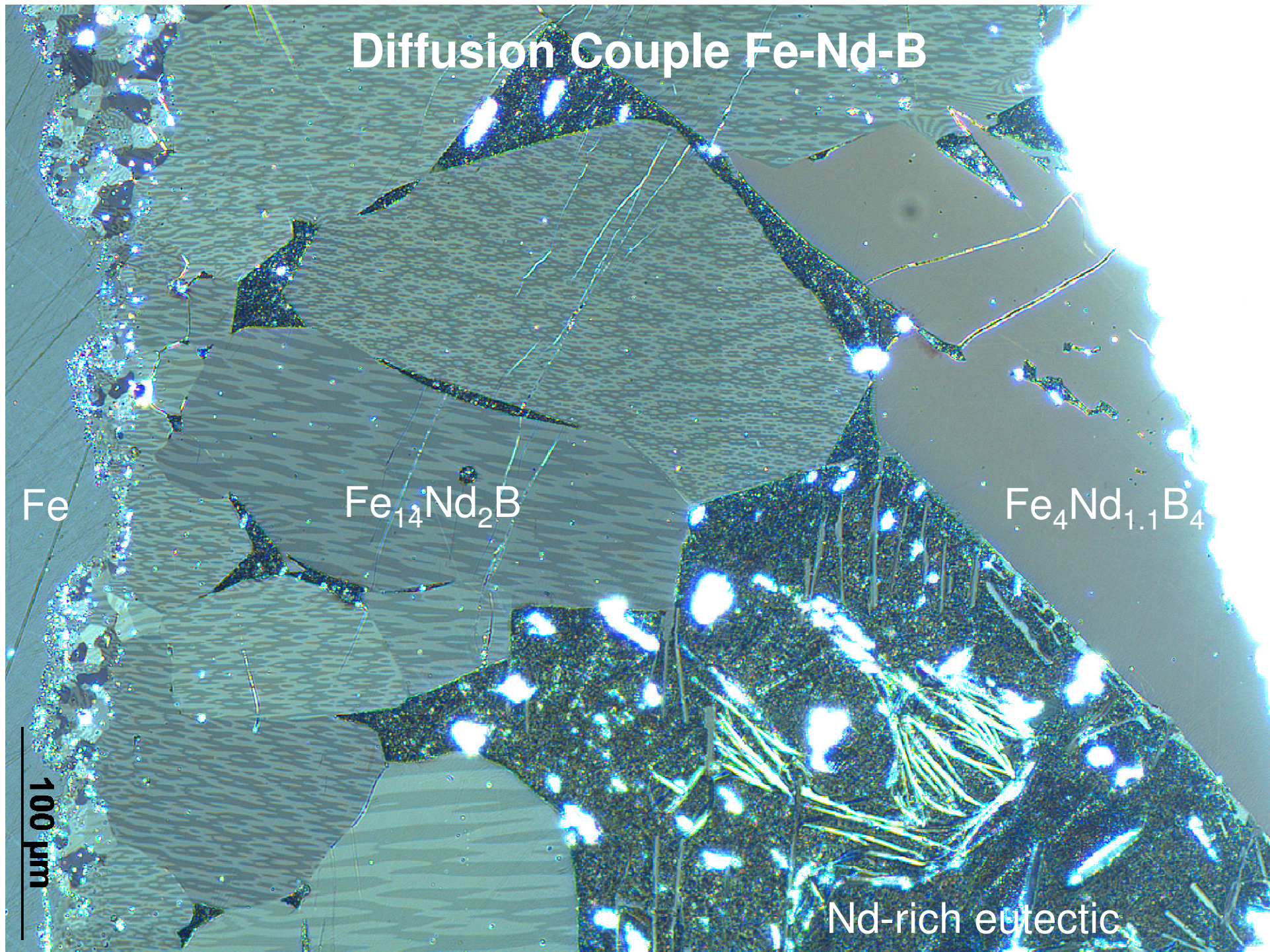
Fe

$\text{Fe}_{14}\text{Nd}_2\text{B}$

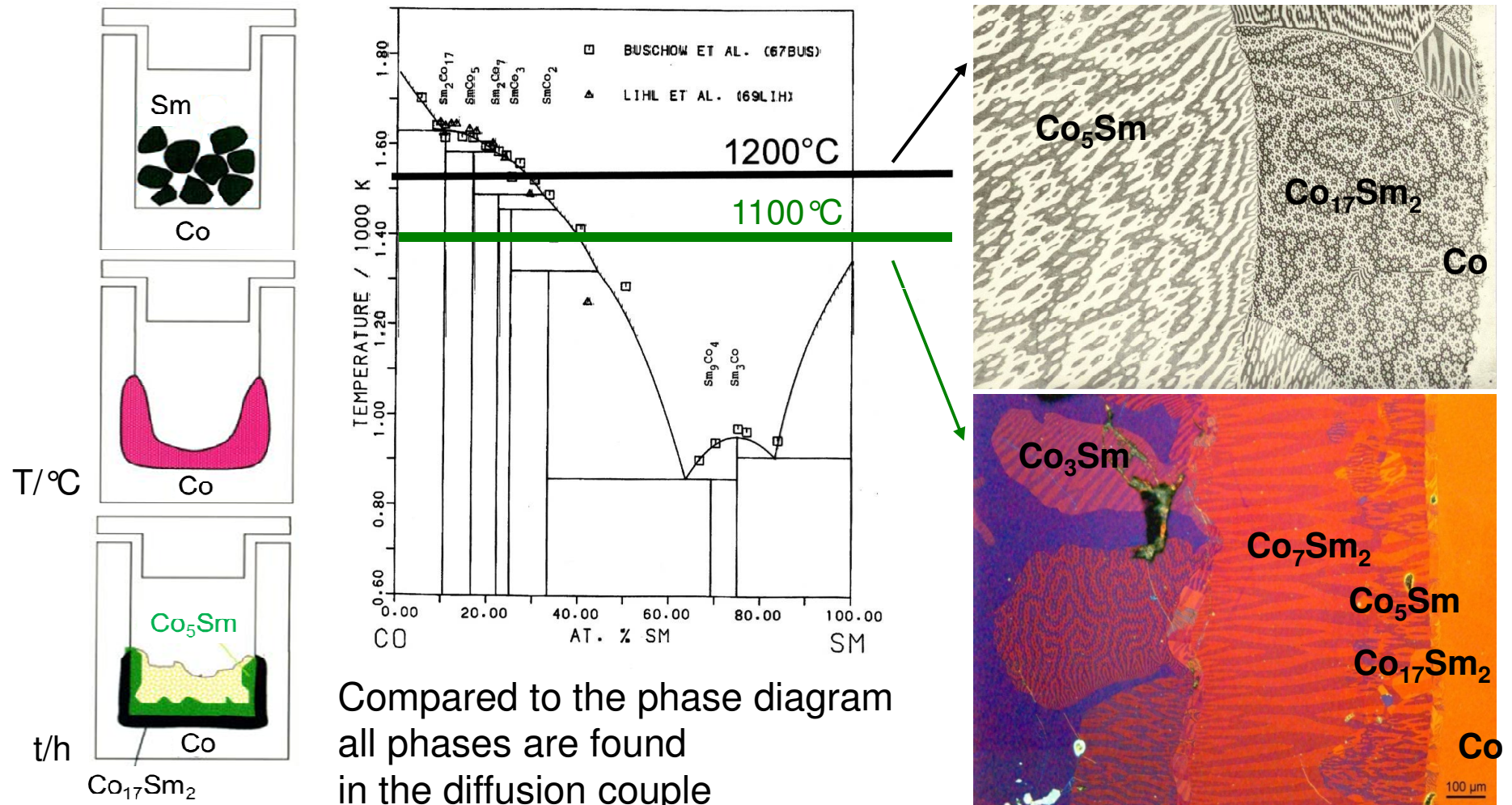
$\text{Fe}_4\text{Nd}_{1.1}\text{B}_4$

100 μm

Nd-rich eutectic



Diffusion Couple – Binary System Co-Sm



Diffusion Couple – Binary System Fe-Nd

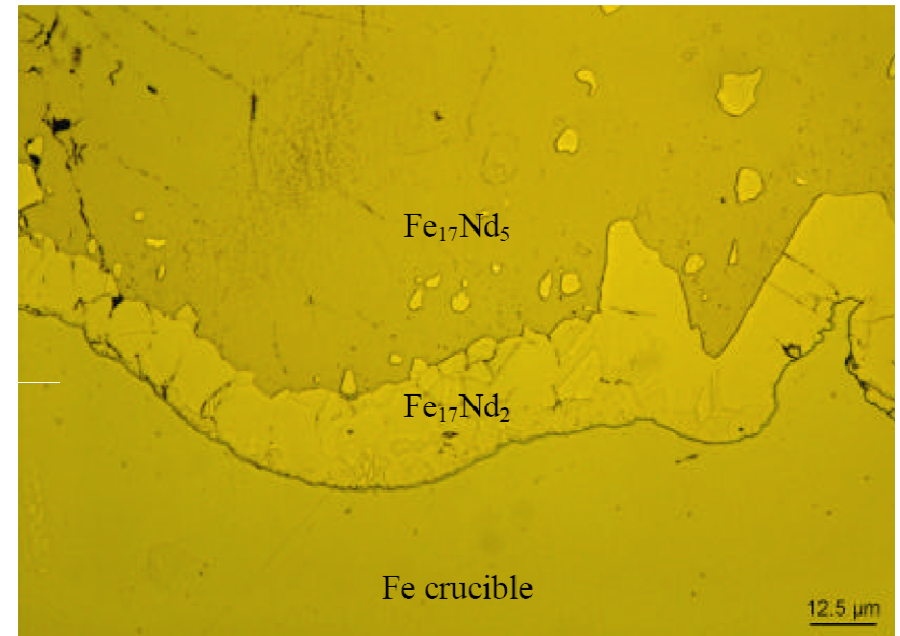
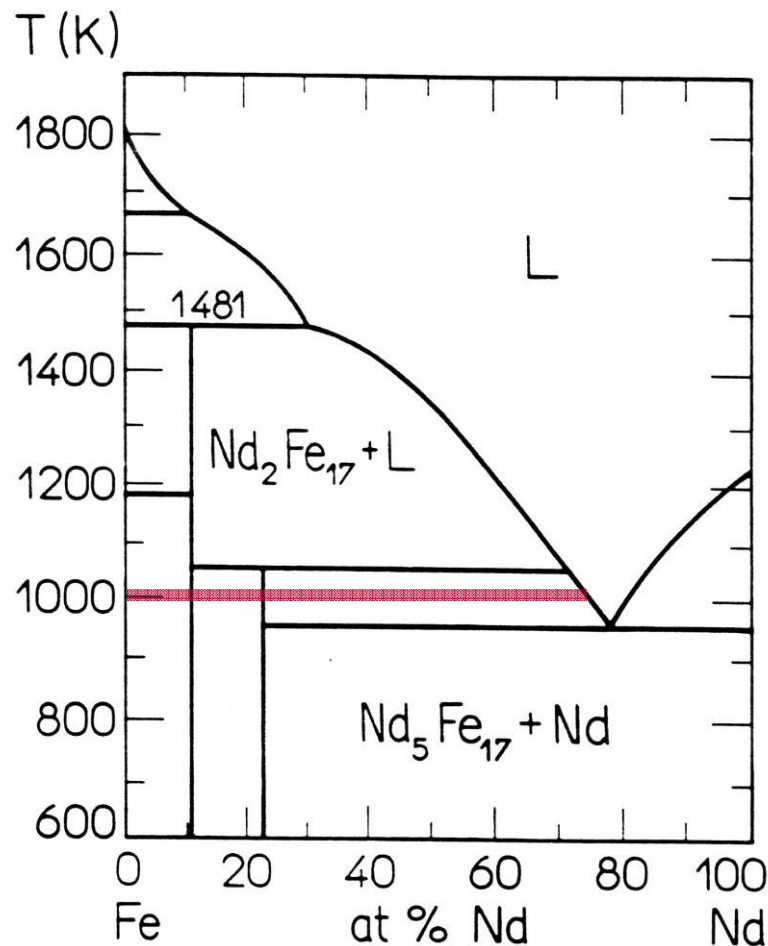
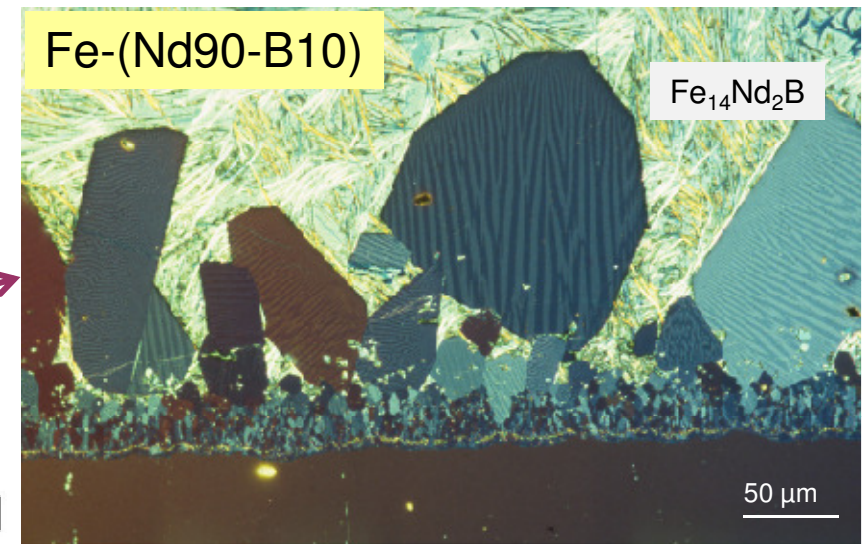
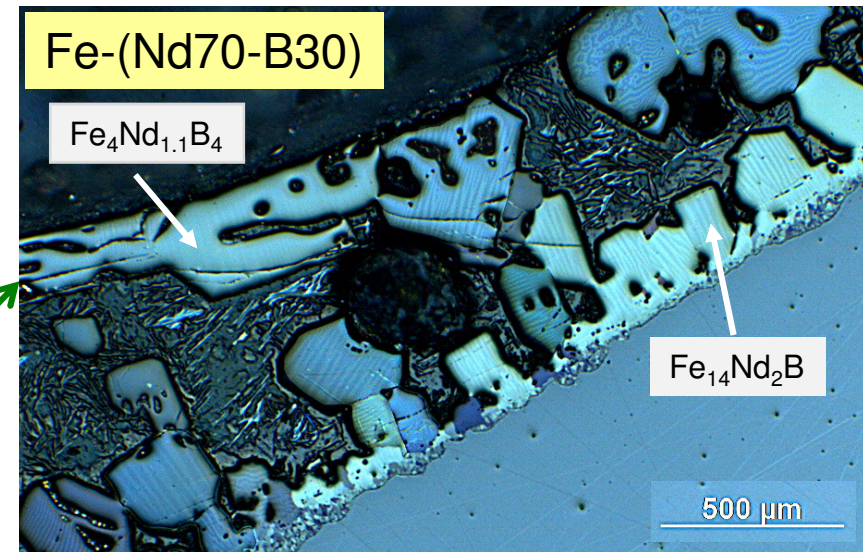
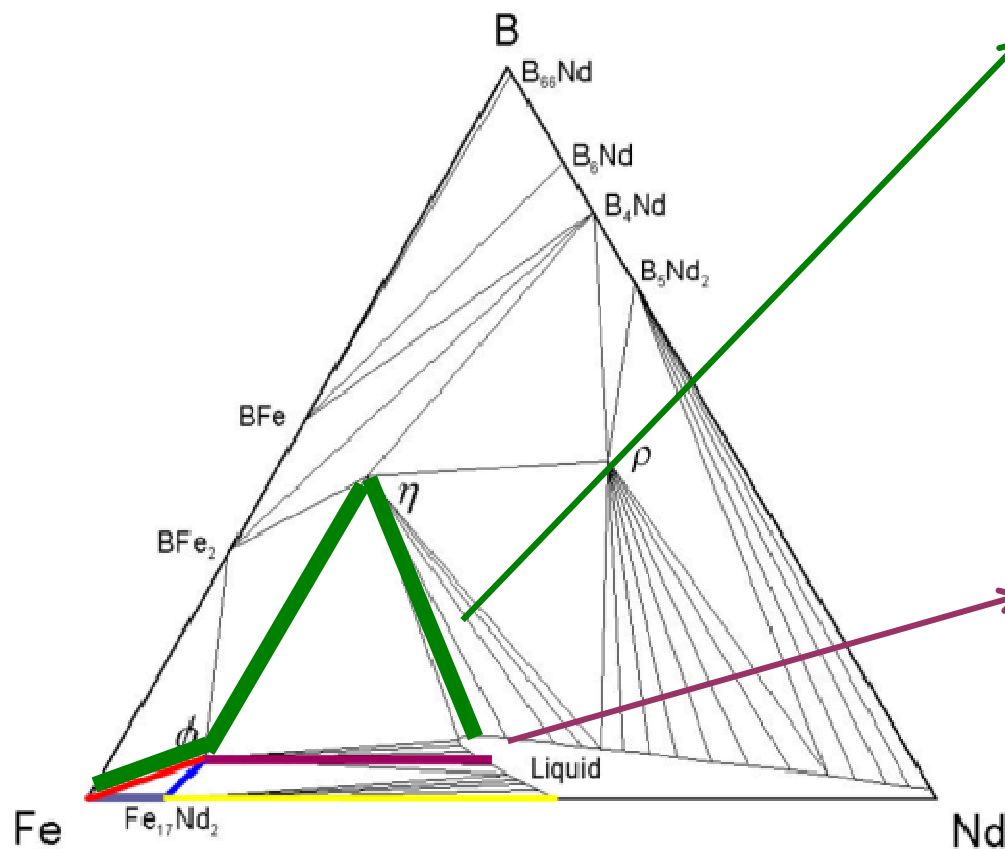
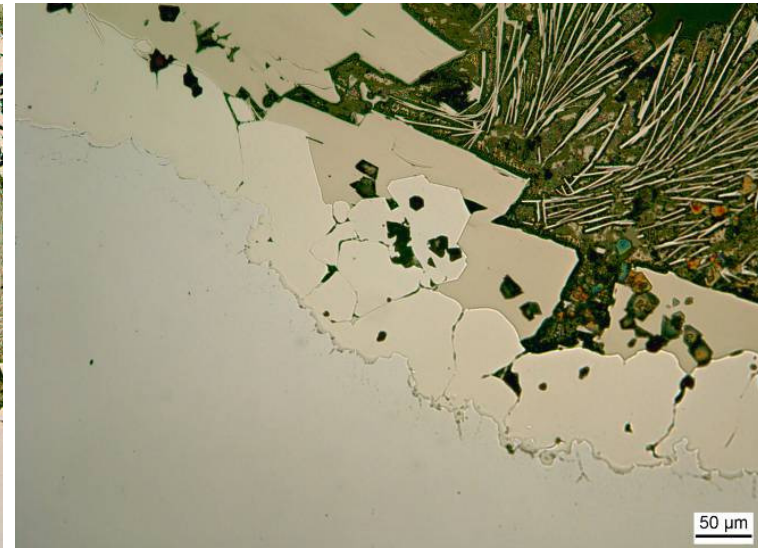
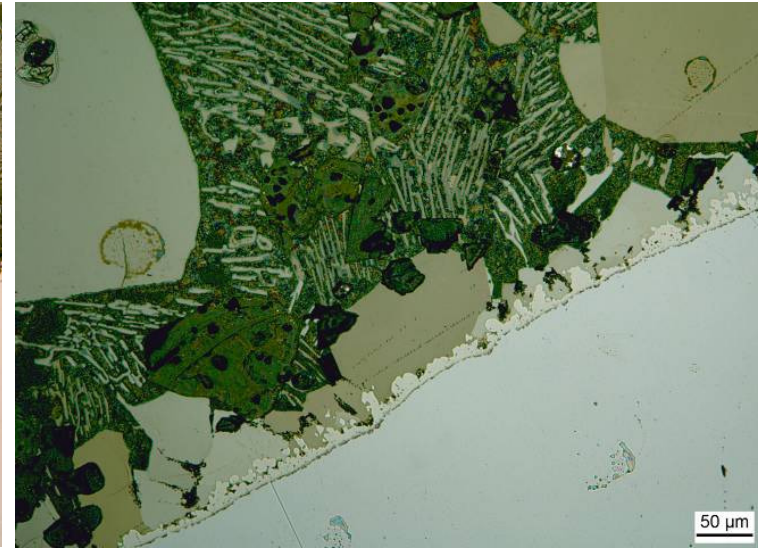
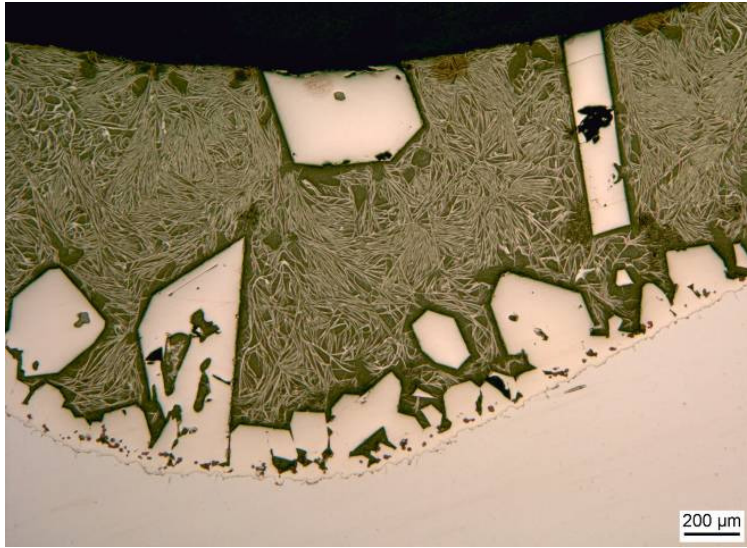


Figure 6.5: Bright field micrograph of an Fe-(Nd100) diffusion couple after a 1050°C heat treatment for 10 hours and 725°C for 30 days. For a better separation between the iron crucible (bottom), the $Fe_{17}Nd_2$ phase (middle) and the $Fe_{17}Nd_5$ phase (top) the specimen was etched with Nital.

Diffusion Couple – Ternary System Fe-(Nd-B)



Examples of Diffusion Couples – 400 in total



Efficient analysis: Search for new magnetic phases

- High-throughput
- Determination of the intrinsic magnetic properties
- Characterization of intrinsic properties in small crystals (J_S , K_1 , T_C)

Optical microscope
Phases



Kerr microscope
Magnetic phases



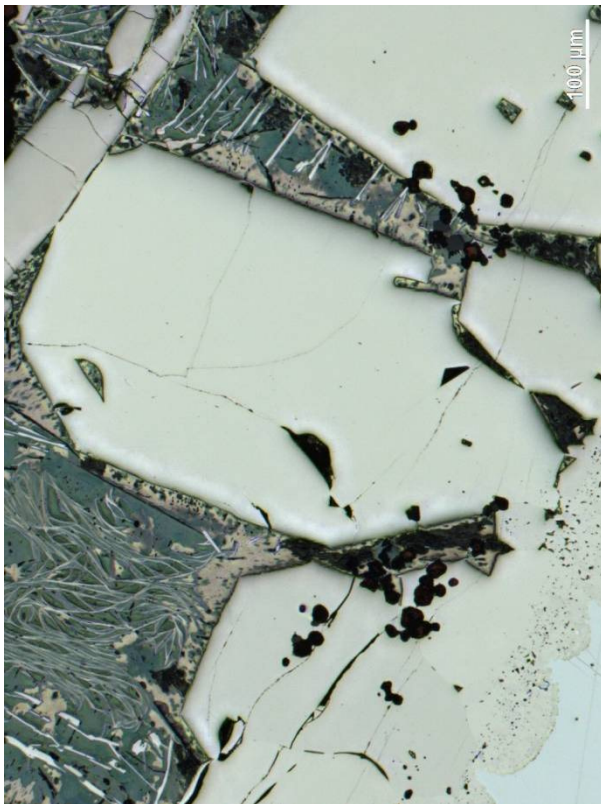
Electron microscope
Chem. composition



Efficient analysis: Search for new magnetic phases

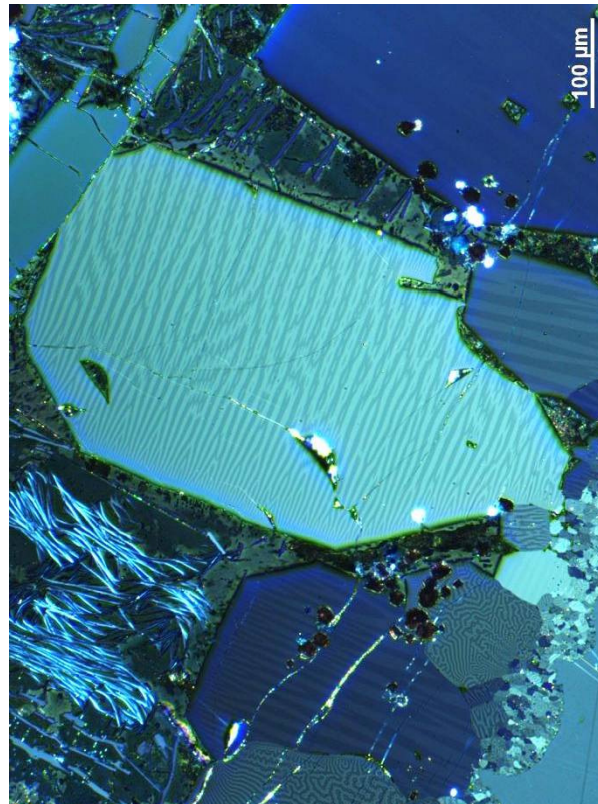
- Correlative microscopy, quantitative microstructure analysis (QMA)

Optical microscopy



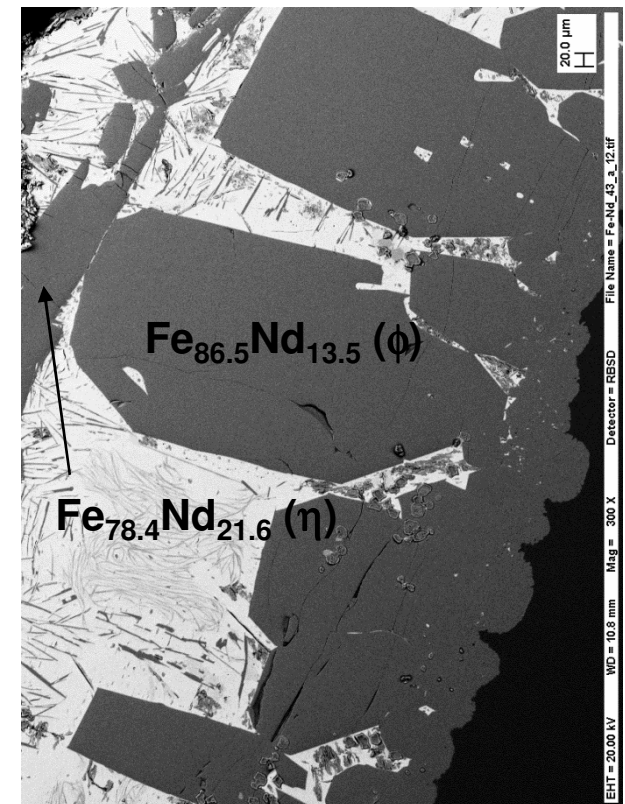
Identification of different phases

Kerr microscopy



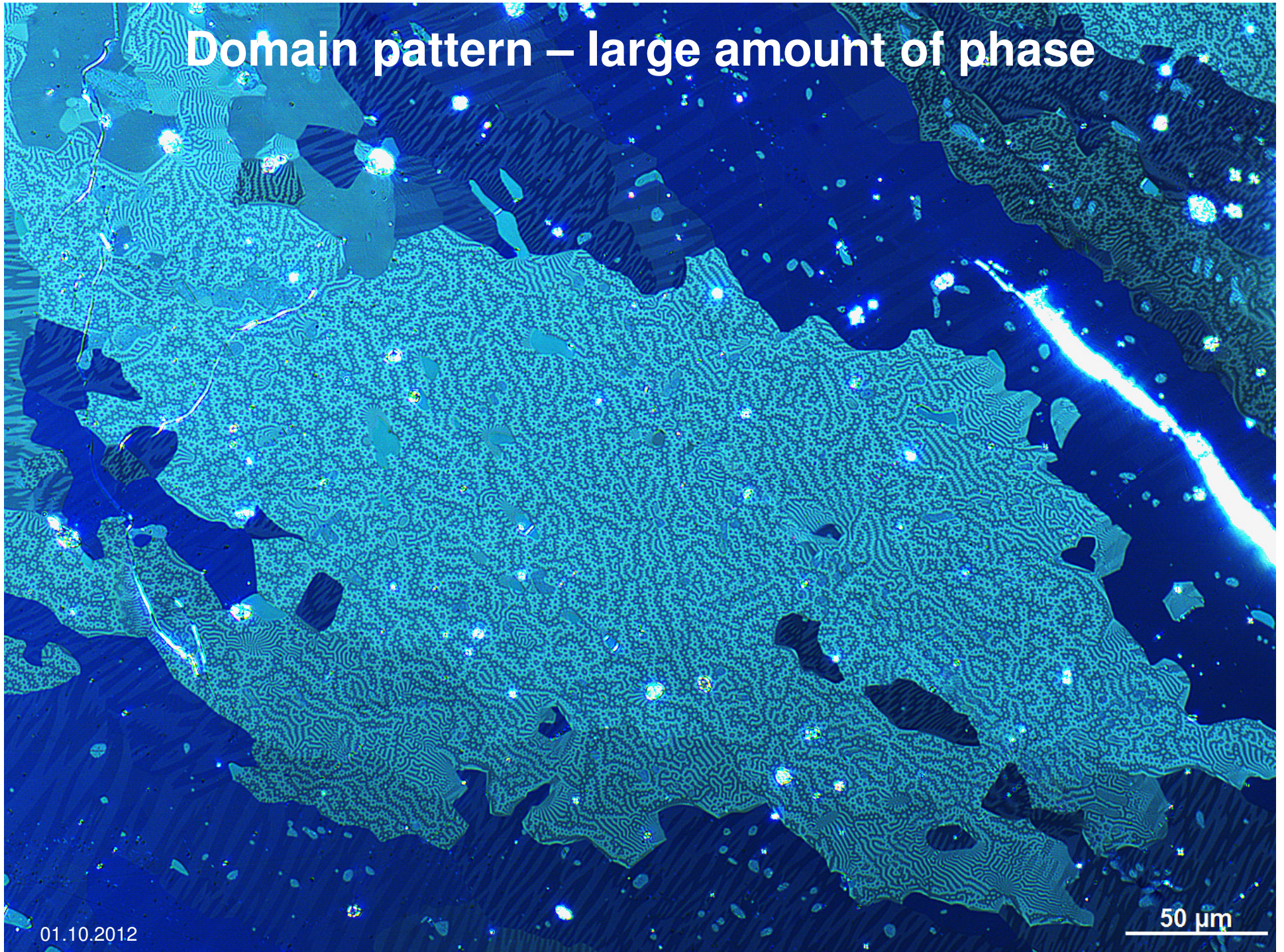
Identification of magnetic phases

REM / EDX

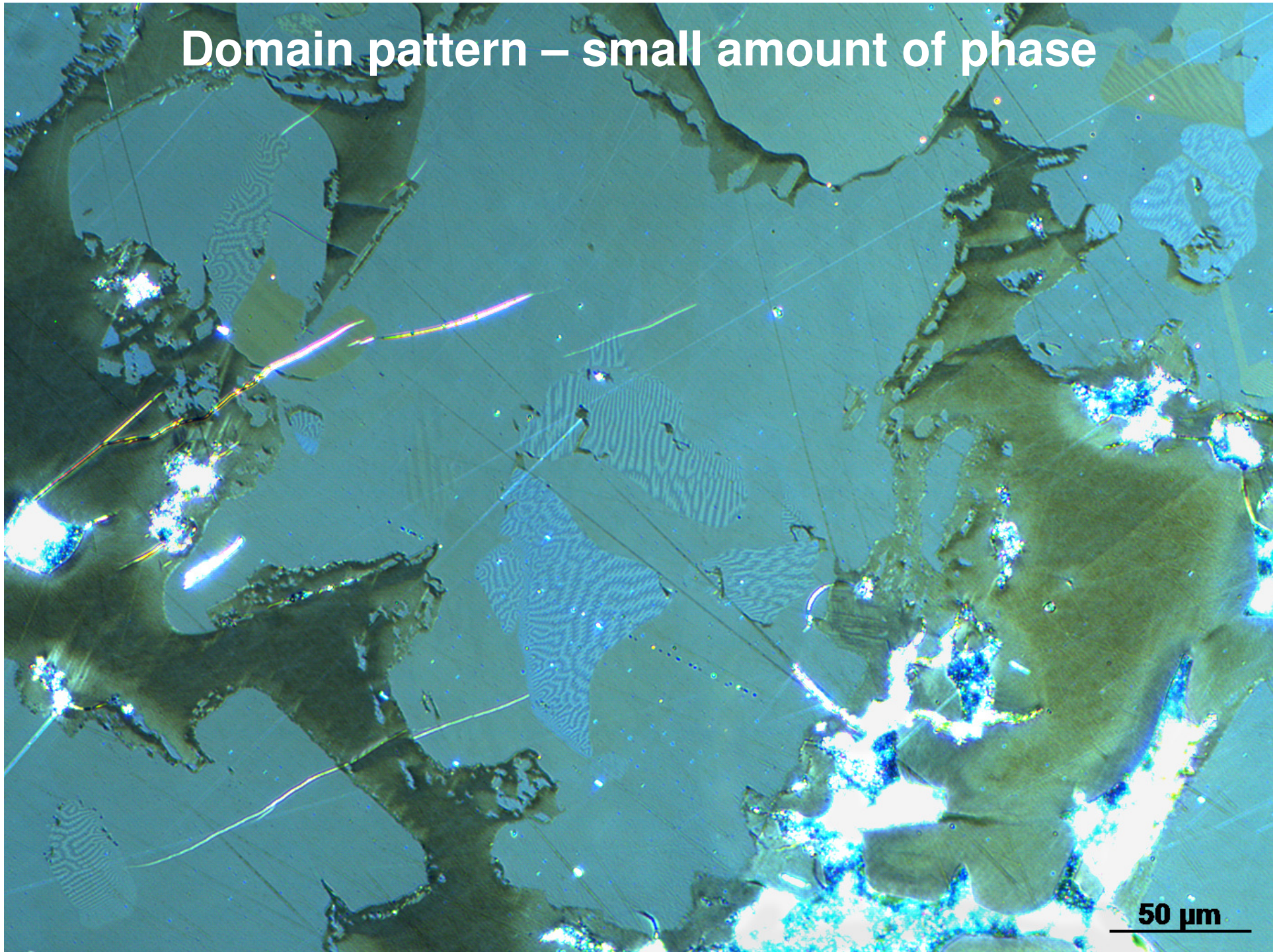


Determination of the chemical composition

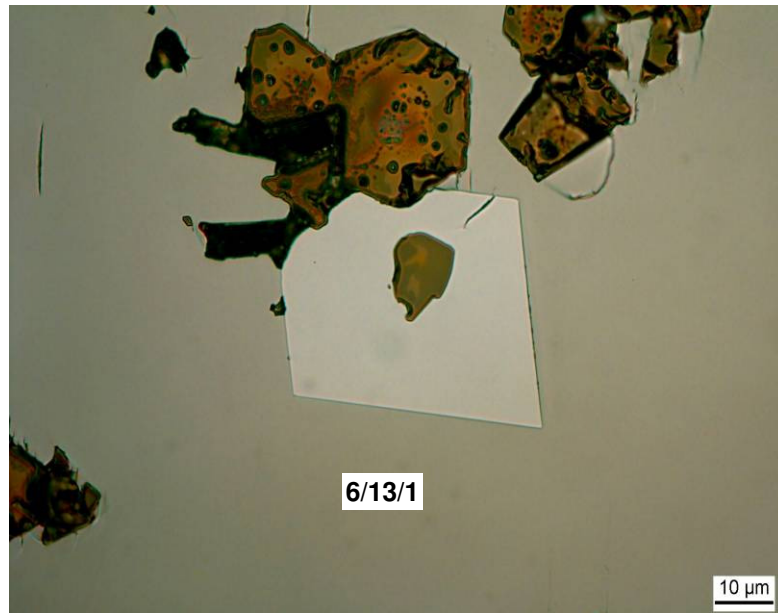
Domain pattern – large amount of phase



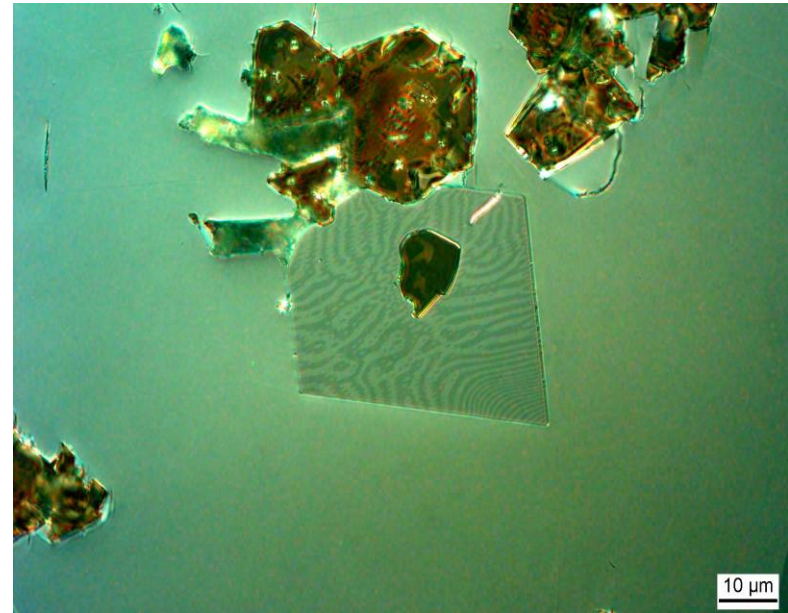
Domain pattern – small amount of phase



Ternary Fe-Pr-Mn-System

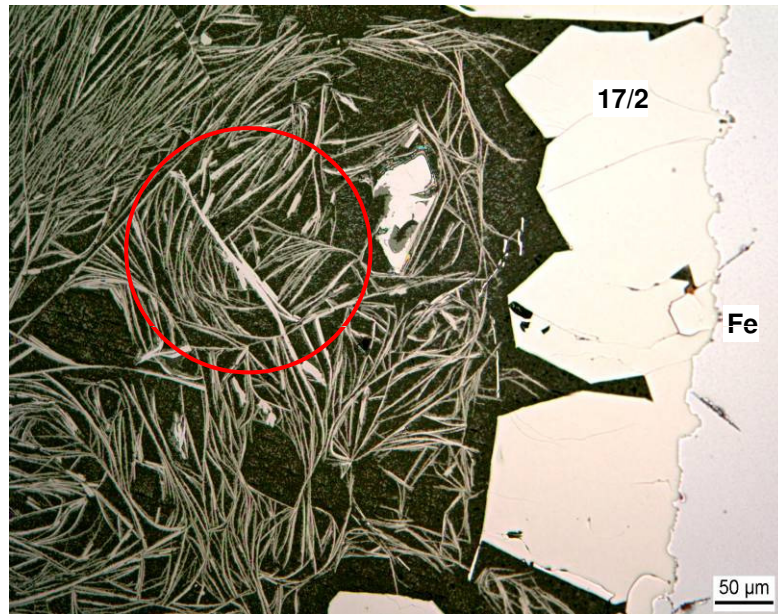


Photomicrograph of an unknown crystal surrounded by the 6/13/1 phase.

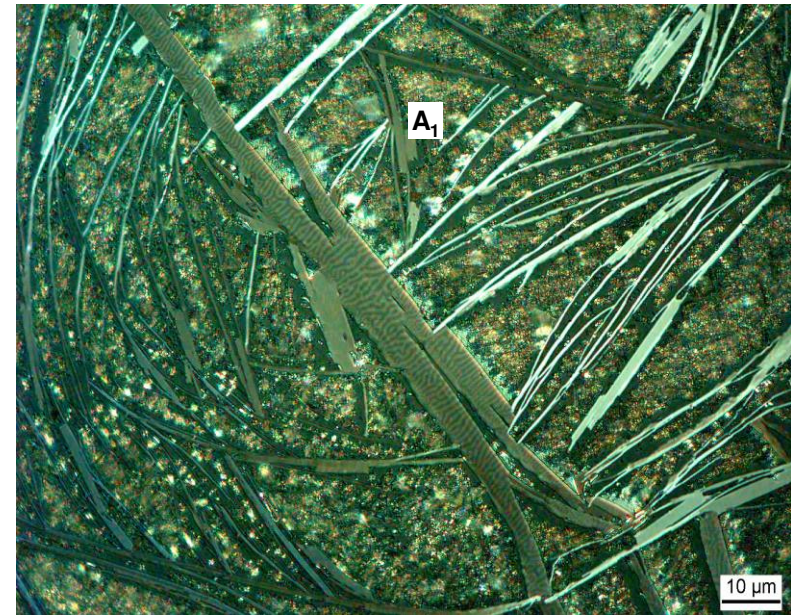


Optical micrograph in polarized light of the unknown crystal with uniaxial domain structure

Diffusion Couple Fe-(Pr₉₀-Na₁₀) Heat Treated at 1050 °C / 10h



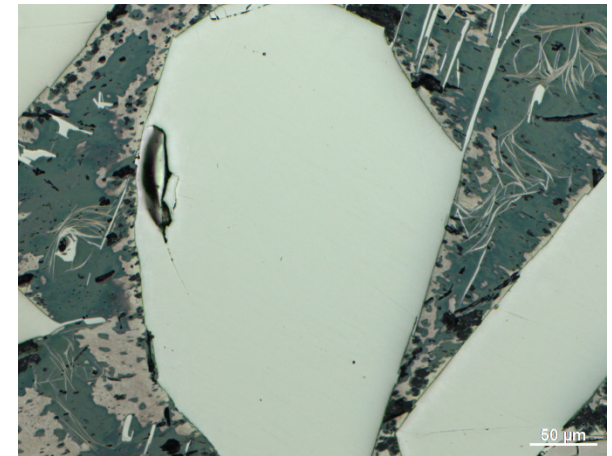
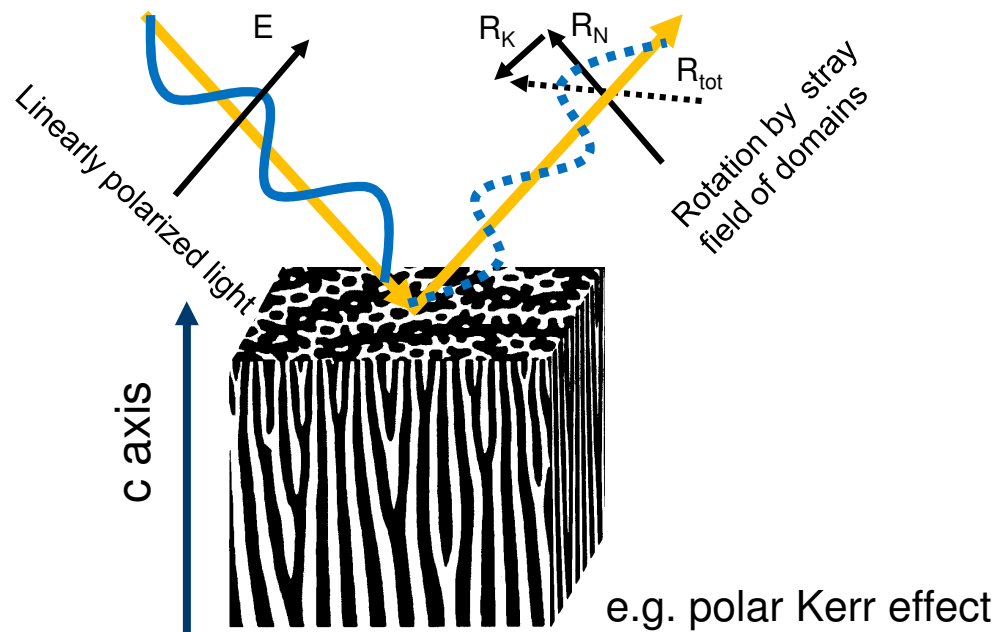
Optical micrograph of the 17/2 phase and the eutectic.



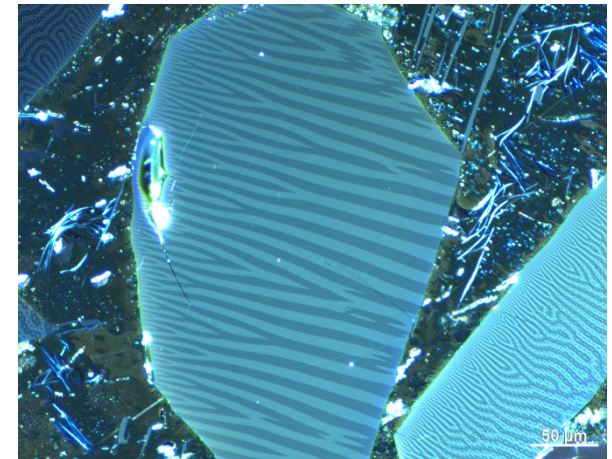
Optical micrograph in polarized light of the A₁ phase with domain pattern.

Kerr effect using the example of $\text{Nd}_2\text{Fe}_{14}\text{B}$

- Linearly polarized light
- Magnetic field rotates plane of polarization ($R_{\text{tot}} = R_N + R_K$)
- Visualization of domains by analysator
- Domain contrast depending on magnetization

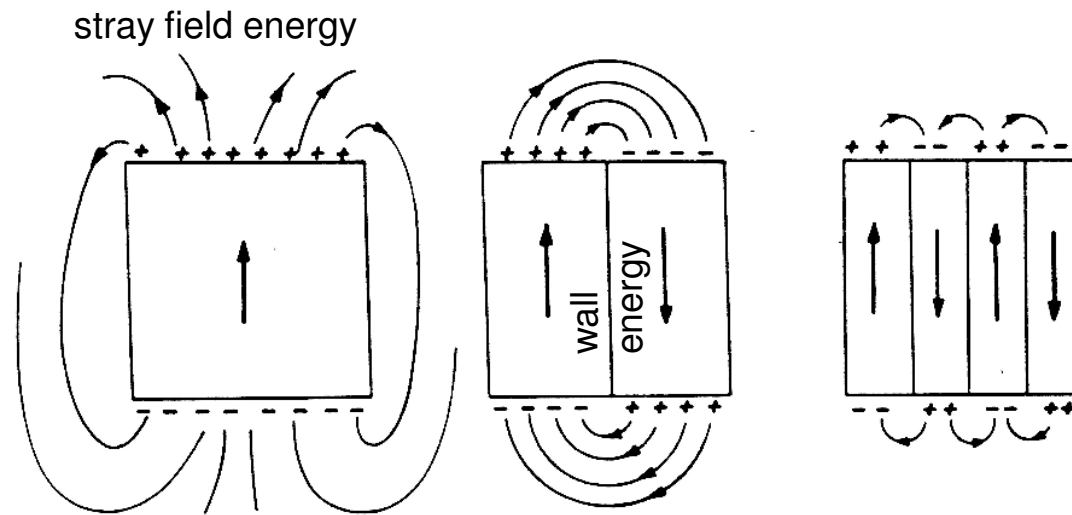


Bright field image, 200x

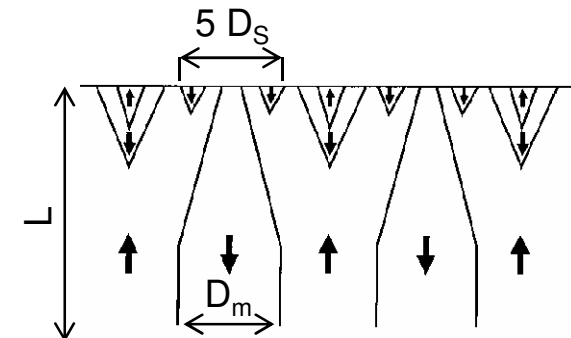


Kerr image, 200x

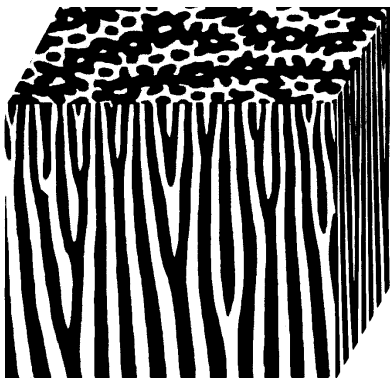
Domain pattern for uniaxial anisotropy ($\text{Nd}_2\text{Fe}_{14}\text{B}$)



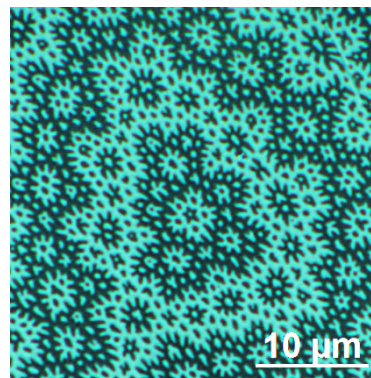
Minimization stray field energy by reversed spikes



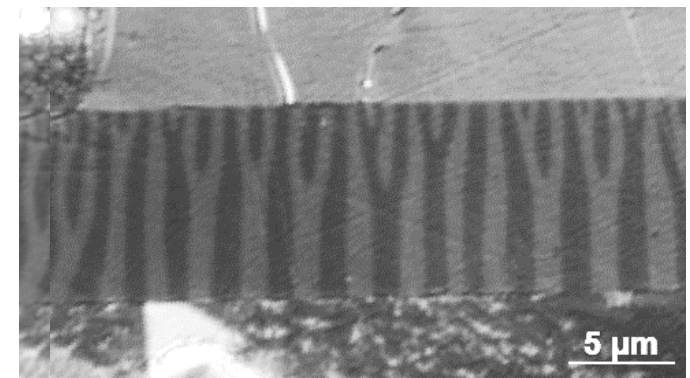
D_m : domain width
 L : grain thickness



3D-model

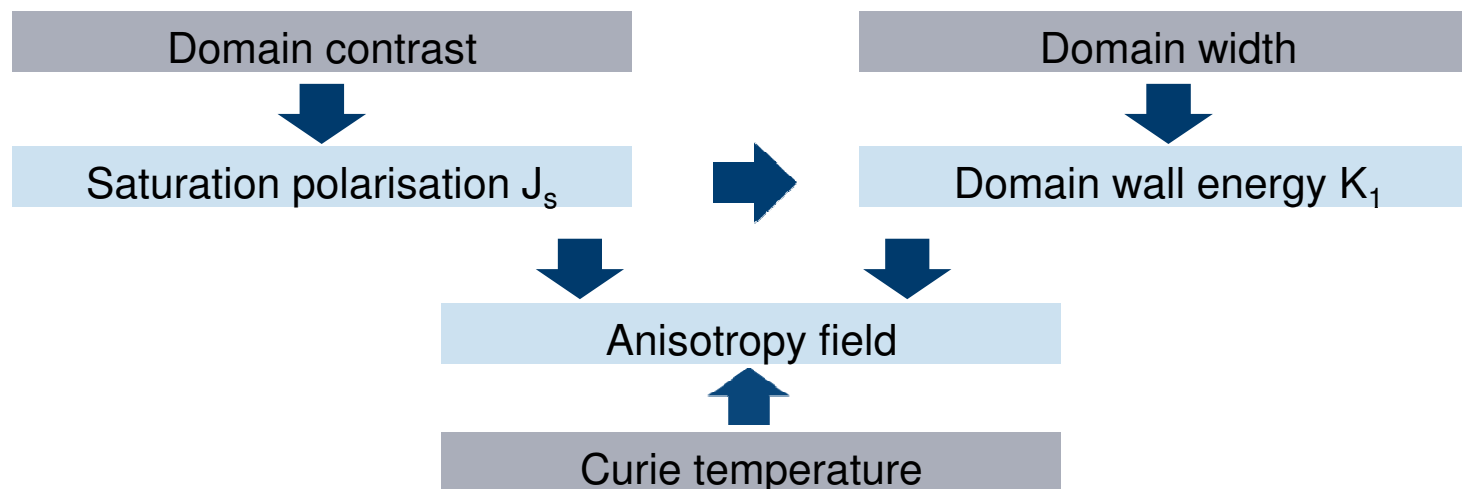
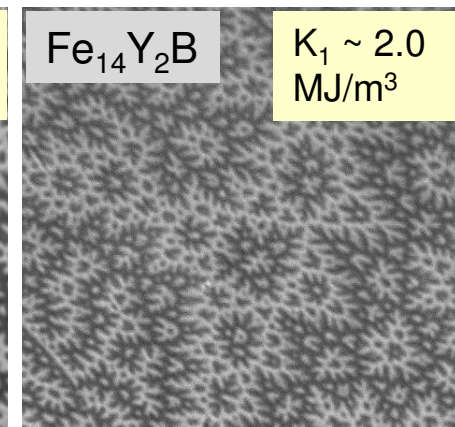
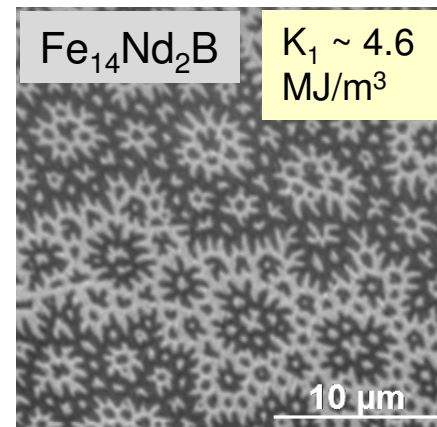
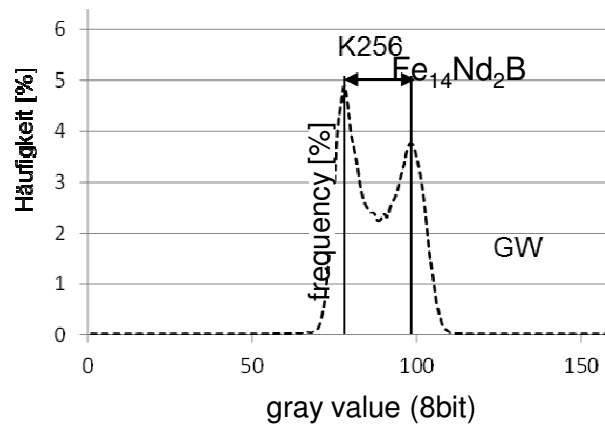


closure domain with reversed spikes

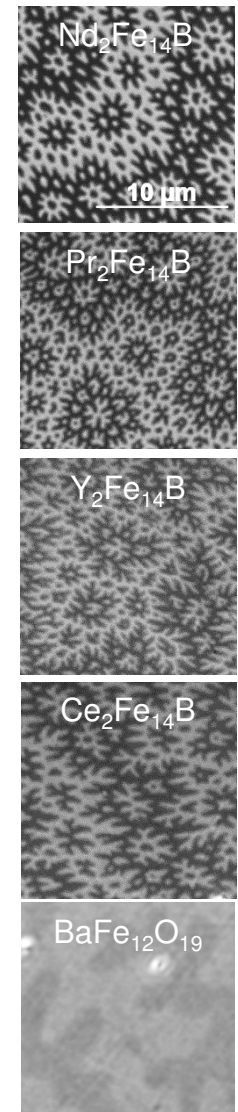
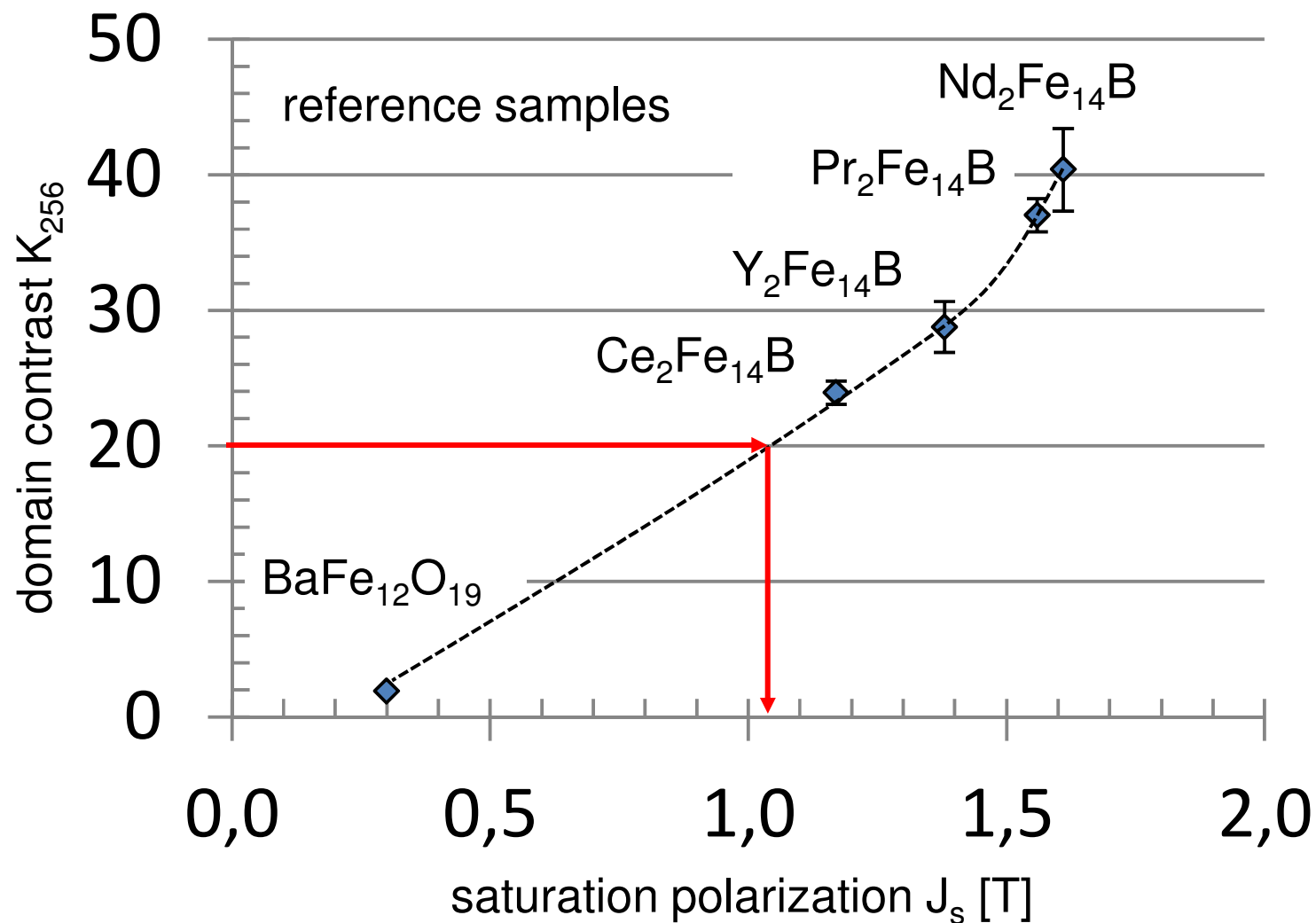


stripe domain with branching

Relationship between domain pattern and intrinsic magnetic properties



Saturation polarization J_s from domain contrast



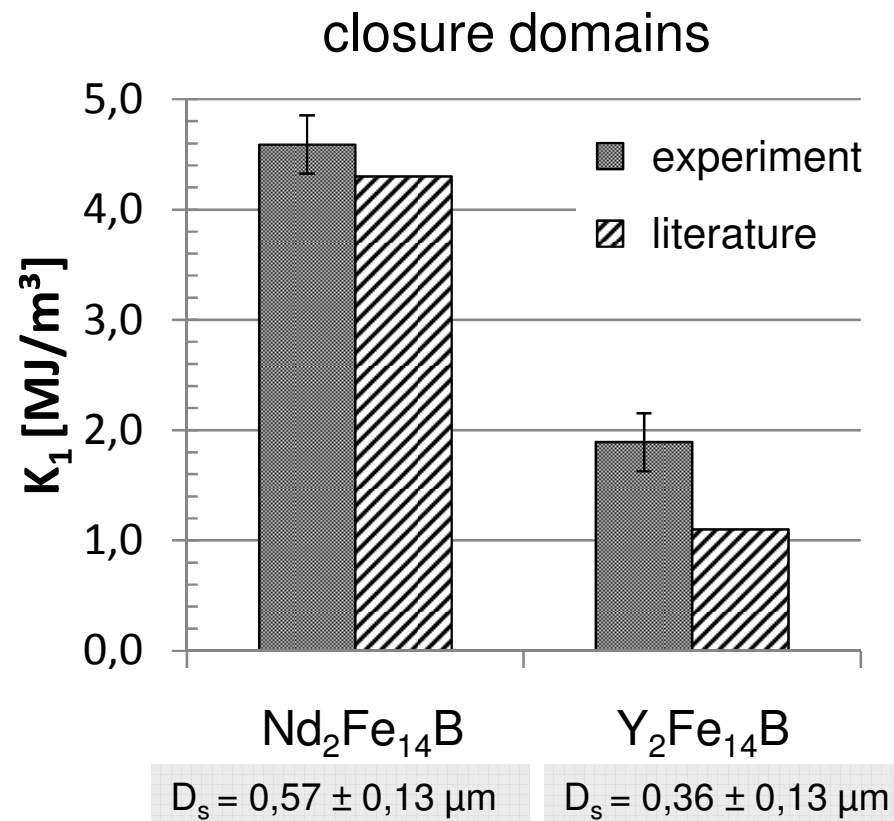
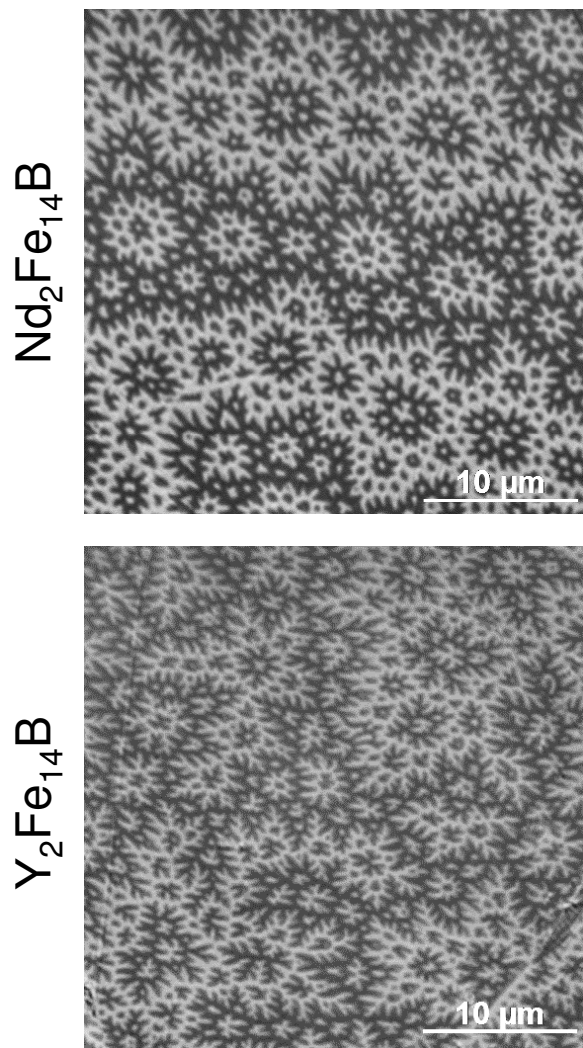
Anisotropy constant K_1 from domain width

- Different models for determination of K_1

| Domain pattern | Formula | Reference |
|---|---|---|
| stripe domain for grain thickness $< 10 \mu\text{m}$ | $D_m = (\gamma L / 1.7 M_S^2)^{1/2}$ | [Kit46] C. Kittel, Phys. Rev. 70, 965 (1946) |
| stripe domain, for grain thickness $> 10 \mu\text{m}$ | $D_m = 0.395(\gamma \mu^* / M_S^2)^{1/3} L^{2/3}$ | [Szy73] R. Szymczak, Acta Phys. Pol. A 43, 571 (1973) |
| closure domain, for grain thickness $> 80 \mu\text{m}$ | $D_s = \beta 4\pi \gamma / M_S^2$ | [Bod77] R. Bodenberger, A. Hubert, Phys. Stat. Sol. (a) 44, K7-K11 (1977) |

- Wall energy $\gamma = 4(AK_1)^{1/2}$, with exchange constant $A \approx 1 \cdot 10^{-11} \text{ J/m}$
- For identical grain thickness phases with larger magnetocrystalline anisotropy show a larger domain width compared to phases with smaller anisotropy constant.

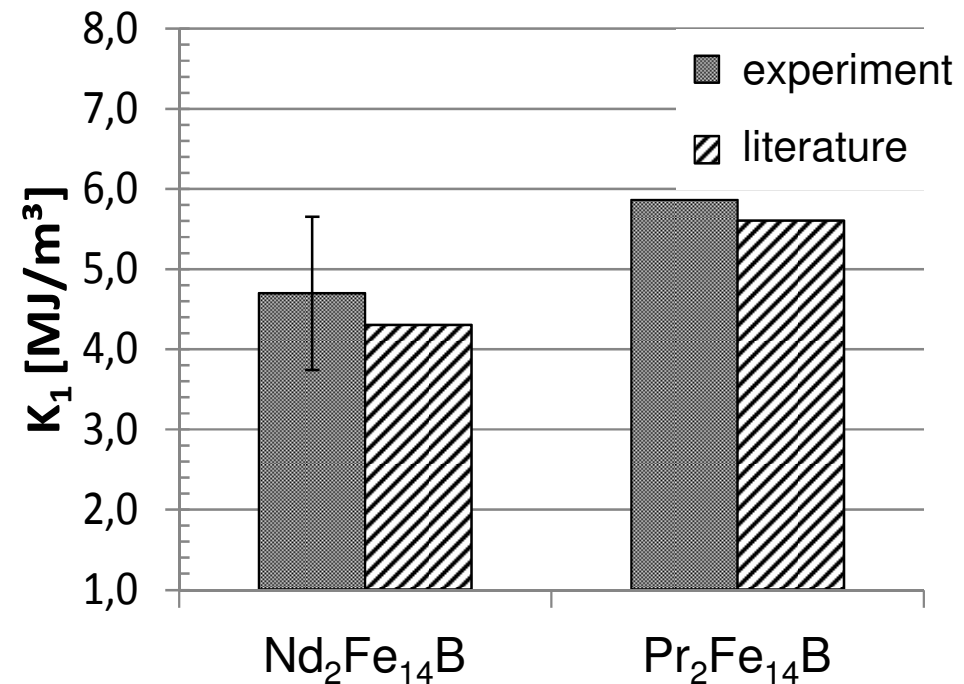
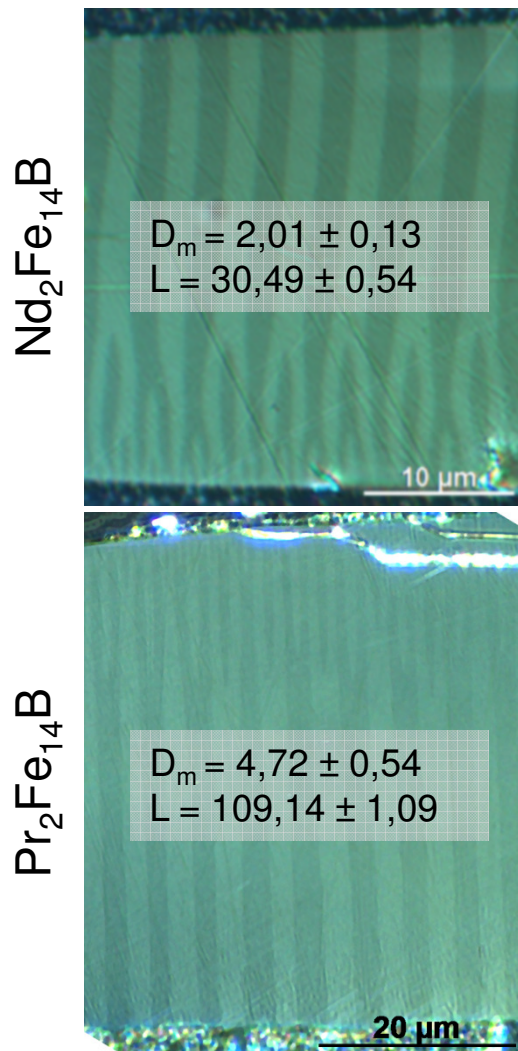
Anisotropy constant K_1 from domain width



$$D_s = \beta 4\pi\gamma / M_s^2 \quad [\text{Bod77}] \quad (\beta = 0.31)$$

Kerr images, 1000x, oil pole

Anisotropy constant K_1 from domain width



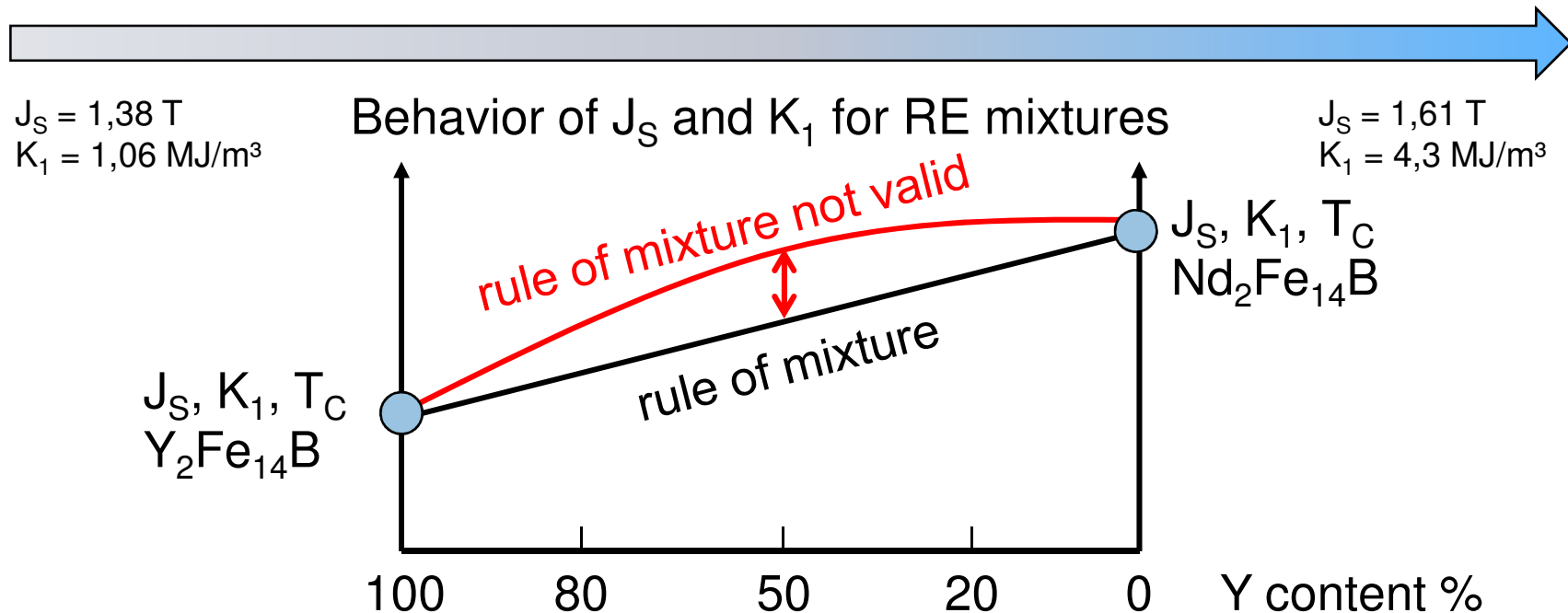
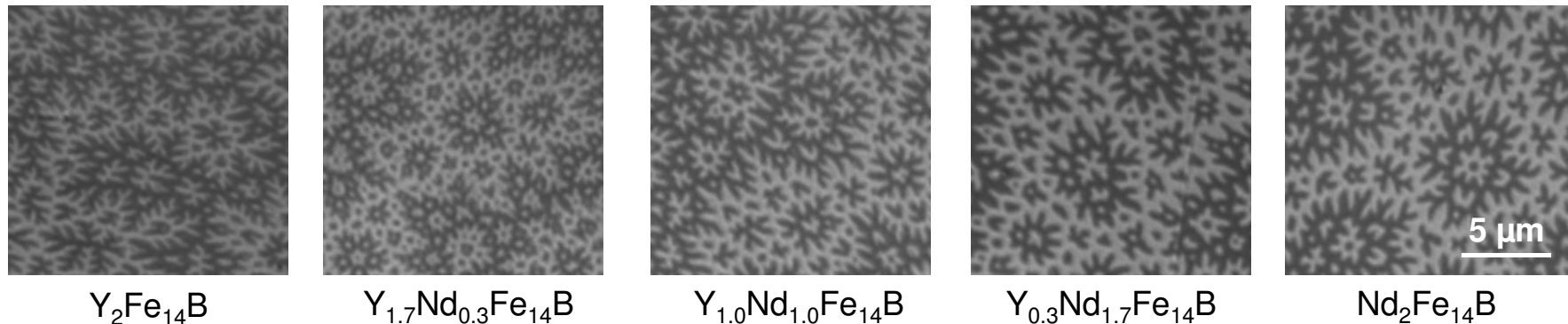
$$D_m = 0.395(\gamma\mu^*/M_S^2)^{1/3} L^{2/3} \text{ [Szy73]}$$

Average grain thickness: L [μm]

Average domain width: D_m [μm]

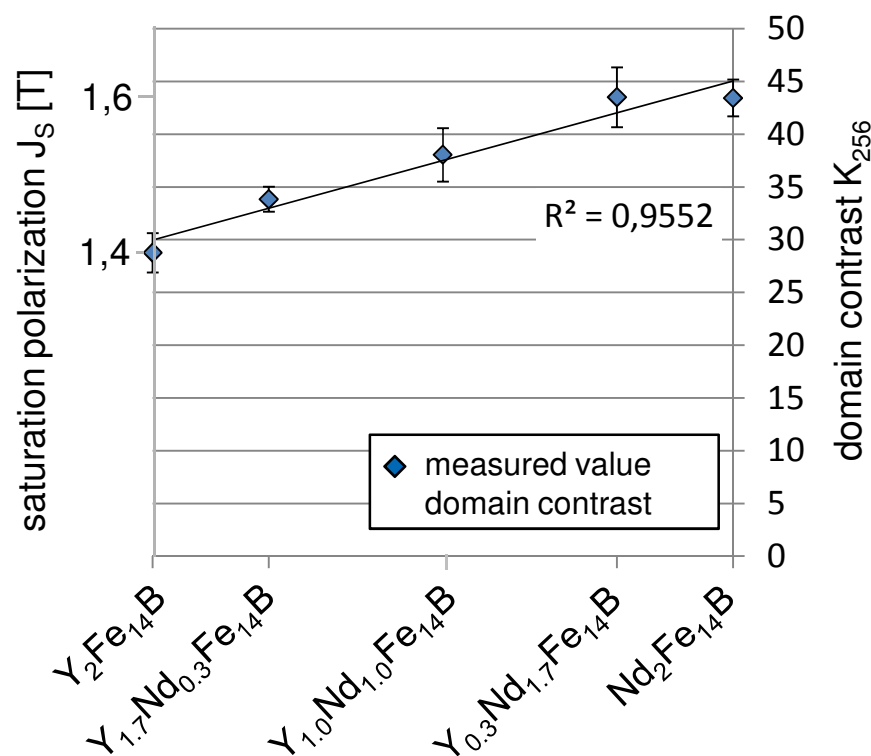
Kerr image, 500x und 1000x oil pole

Example $(Y_{1-x}Nd_x)_2Fe_{14}B$ ($x = 0..1$)

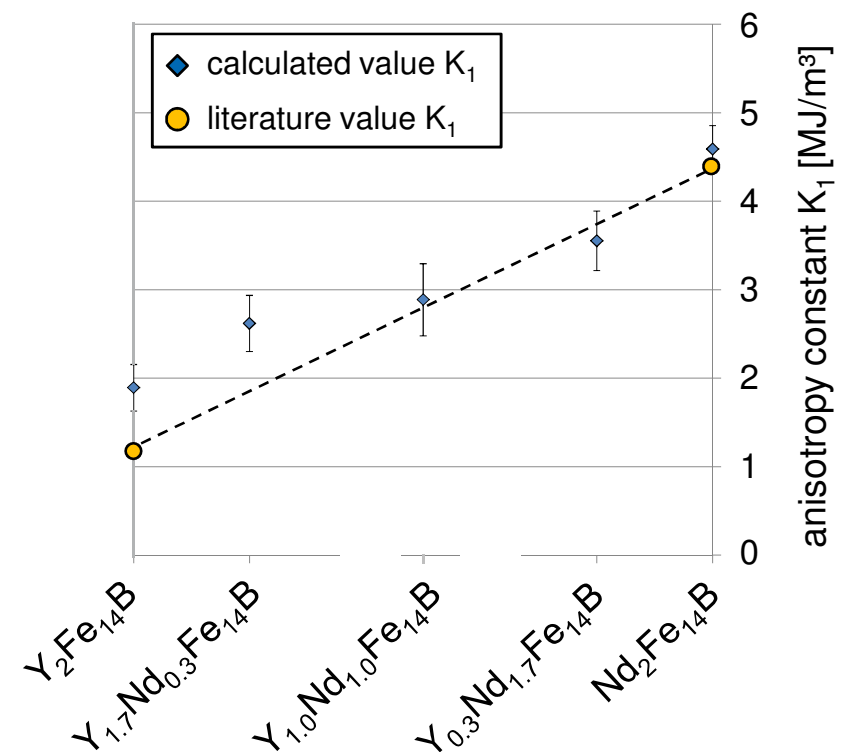


Example $(Y_{1-x}Nd_x)_2Fe_{14}B$ ($x = 0..1$)

- J_s and K_1 as function of ratio Y:Nd



Estimation saturation polarization J_s
based on measured domain contrast



Estimation anisotropy constant K_1 based
on measured domain surface width

Search for new permanent magnetic materials

- High Throughput synthesis and analysis methods established
- Search in about 400 different systems completed
- Existence of phases in TM rich corner documented, some interesting candidates identified
- *Still some work to be done!*
 - *Support by first principle approaches needed*
 - *Crystal structures, chemical composition*
 - *Thermodynamic stabilities*
 - *Magnetic properties*
 - *Collaboration with Peter Gumbsch and Ralf Drautz*
 - *Modeling tools still to be developed*

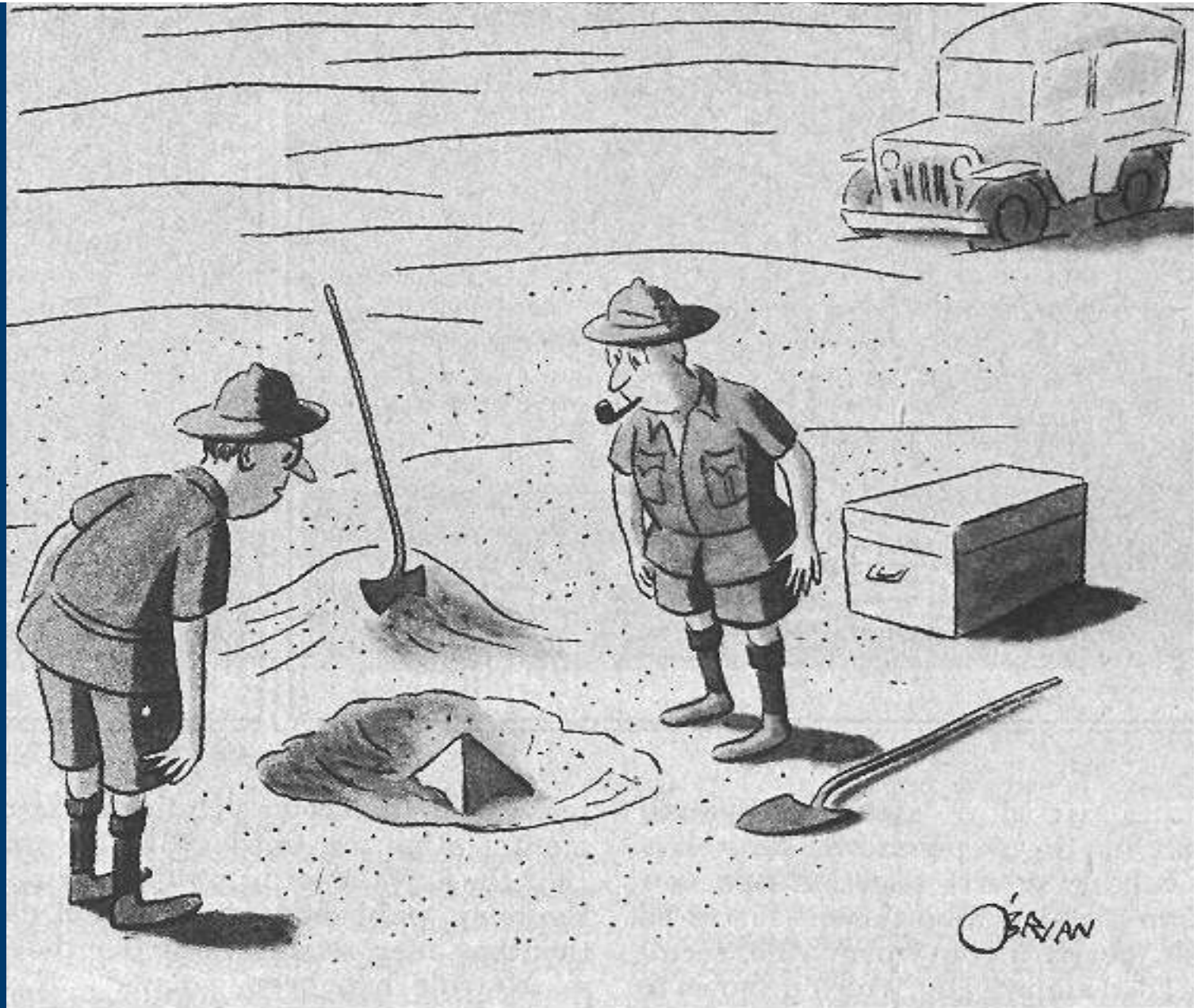
| Diffusion couple | Fe ₁₇ Sm ₂ | Fe ₃ Sm | Fe ₂ Sm | Fe ₁₂ Sm | Fe ₂₉ Sm ₃ | Fe ₁₄ Sm ₆ |
|------------------|----------------------------------|--------------------|--------------------|---------------------|----------------------------------|----------------------------------|
| Fe-Sm-Mg | ✗ | ✓strong | ✓weak | | | |
| Fe-Sm-Ti | ✗ | ✓strong | ✓weak | ✓strong | | |
| Fe-Sm-V | ✓weak | ✓strong | ✓weak | ✓strong | | |
| Fe-Sm-Cr | ✗ | ✓strong | ✓weak | | | |
| Fe-Sm-Mn | ✗ | ✓strong | ✓weak | missing | | |
| Fe-Sm-Co | ✓weak | ✓strong | ✓weak | | | |
| Fe-Sm-Ni | ✗ | ✓strong | | | | |
| Fe-Sm-Cu | ✗ | ✓strong | | | | |
| Fe-Sm-Zr | ✗ | ✓strong | ✓weak | | | |
| Fe-Sm-Nb | ✗ | ✓strong | ✓weak | | | |
| Fe-Sm-Mo | ✗ | ✓strong | ✓weak | | missing | |
| Fe-Sm-In | ✓weak | ✓strong | ✓weak | | | |
| Fe-Sm-Sn | ✓strong | | ✓weak | | | ✗ |
| Fe-Sm-Sb | ✓weak | | ✓weak | | | ✗ |
| Fe-Sm-W | ✗ | ✓strong | | missing | | |
| Fe-Sm-Pb | ✗ | | ✗ | | | |

New phase
found

Phase in larger
amount
synthesized and
analyzed

Development of
processing to
realize
microstructure

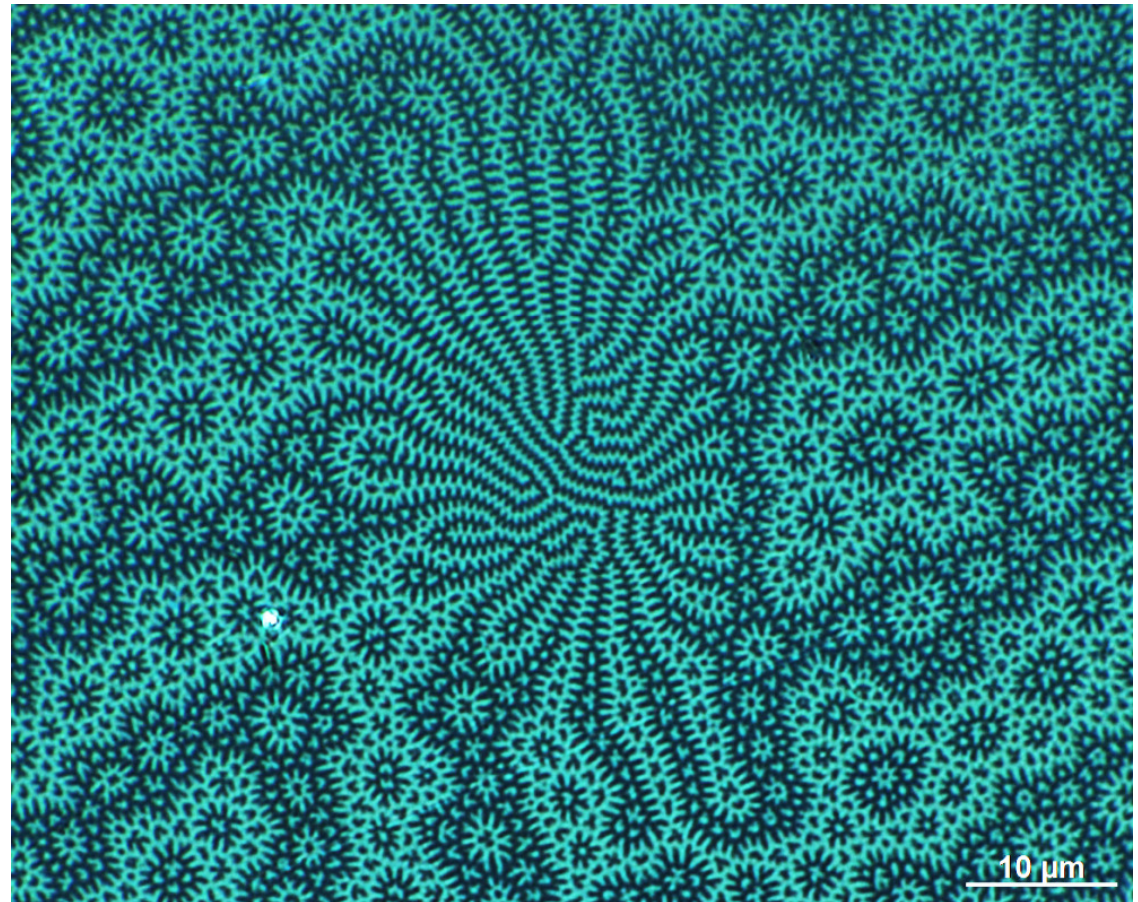
Mass production



"This could be the discovery of the century. Depending of course, on how far down it goes."

Acknowledgements

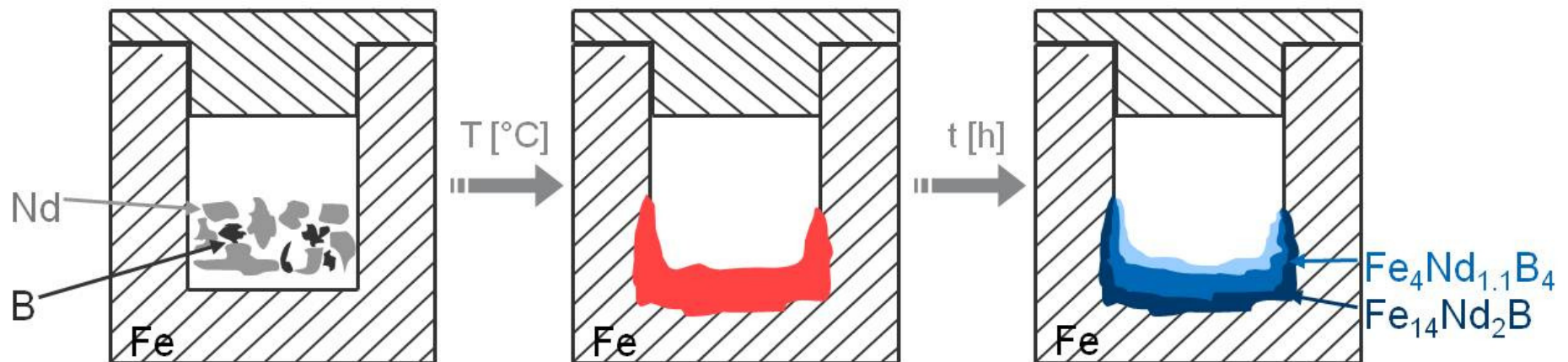
- Bundesministerium für Bildung und Forschung
- Robert Bosch GmbH
- Magnetfabrik Bonn
- Fraunhofer-Institut für Werkstoffmechanik
- Max-Planck-Institut für Intelligente Systeme



Backup

Search for new magnetic phases – efficient synthesis

- High probability to receive numerous phases
- Non-equilibrium states in binary and higher component systems
- Interest focused on TM-rich phases
- Small specimen



The intermetallic phases form during isothermal annealing and during cooling.

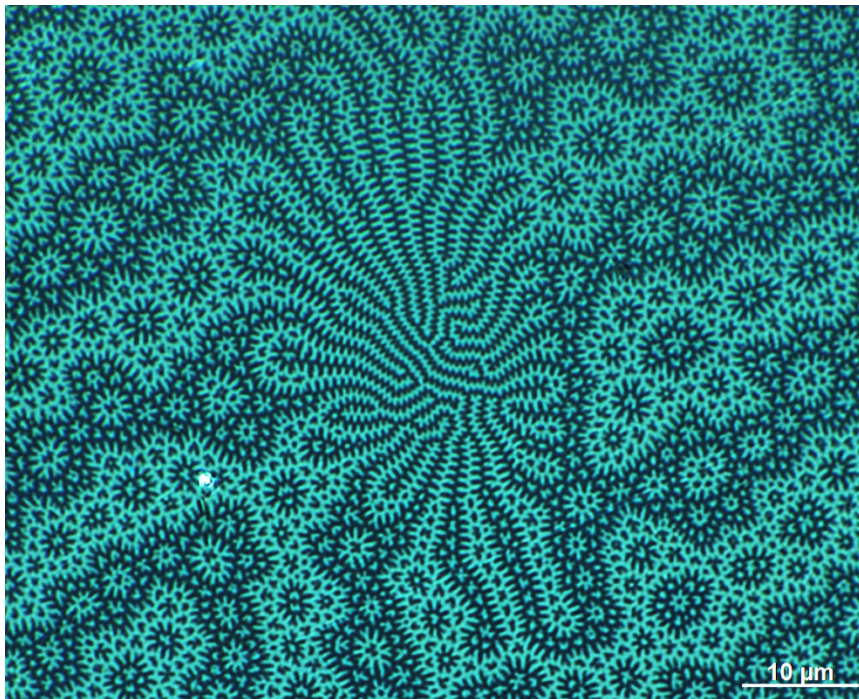
Heterogeneous non-equilibrium states



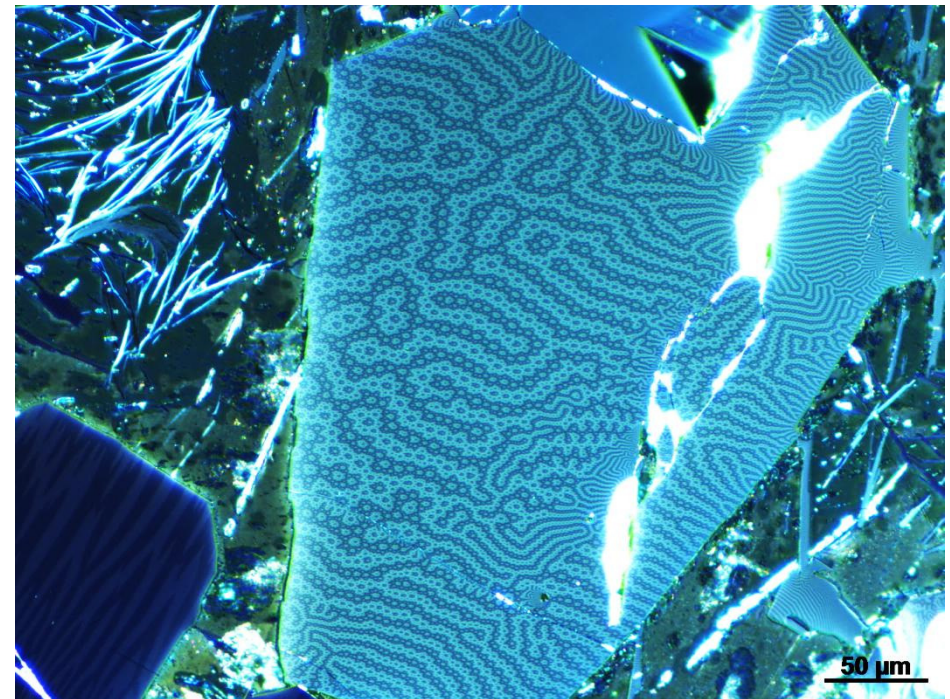
2000 μm

Anisotropy constant K_1 from domain width

- Dependence of domain pattern on grain thickness

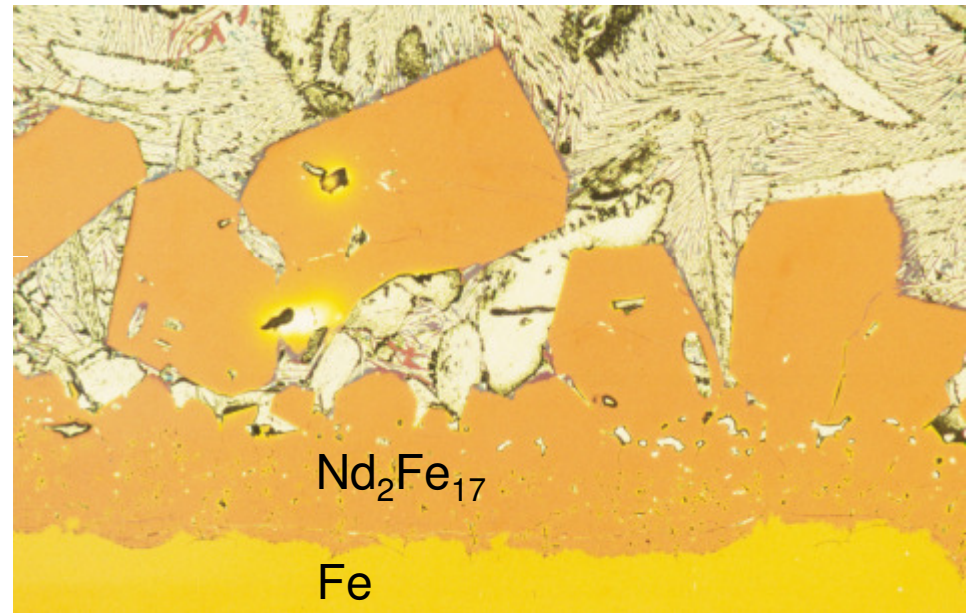
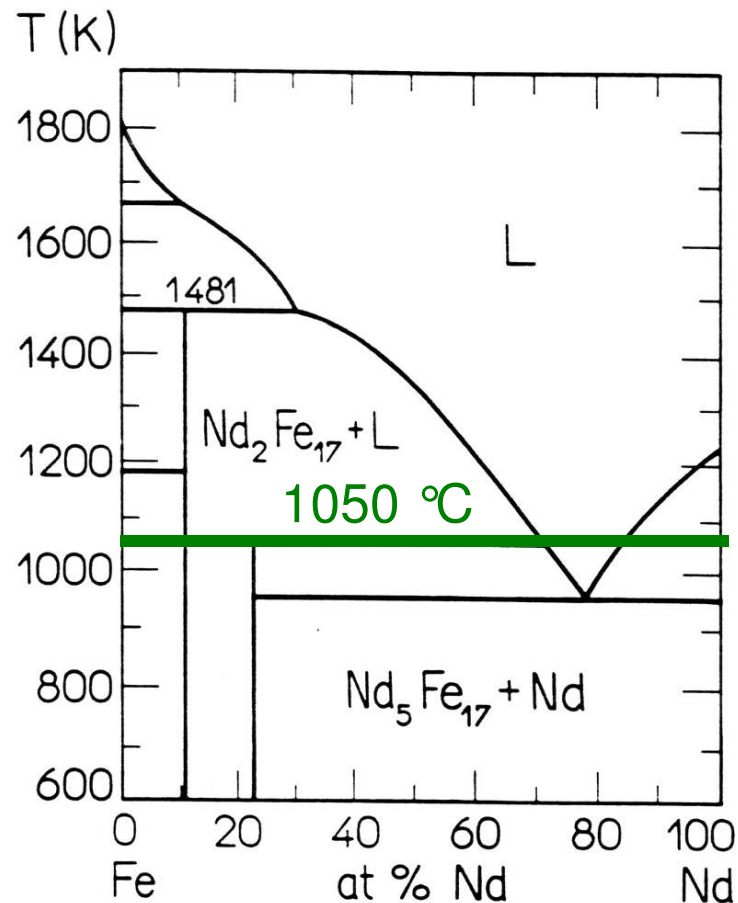


Kerr microscope image
Nd₂Fe₁₄B, 1000x, oil pole



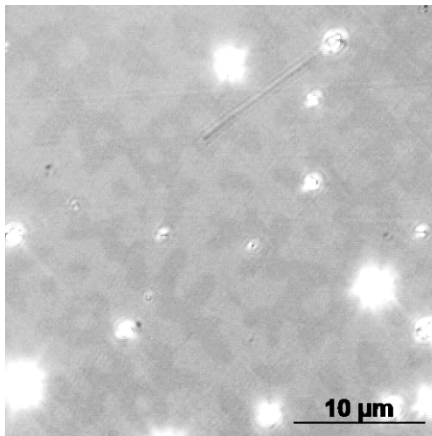
Kerr microscope image
Nd₂Fe₁₄B, 100x

Diffusion Couple – Binary System Fe-Nd

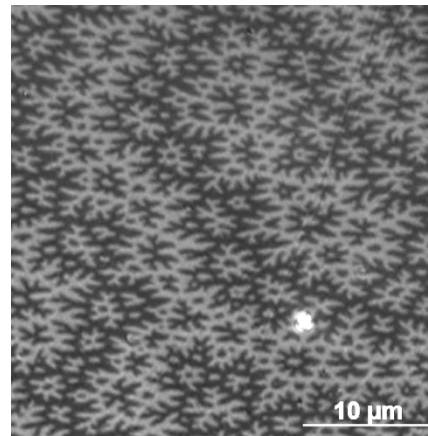


According to the phase diagram all phases are found.

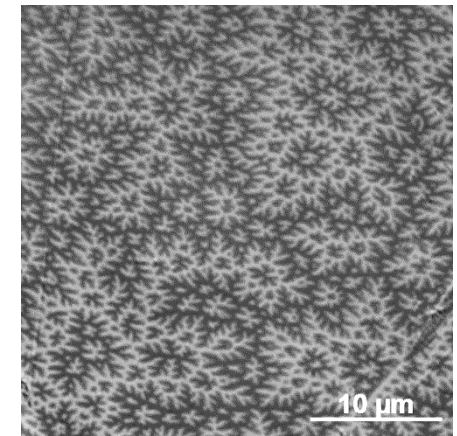
Saturation polarization J_s from domain contrast



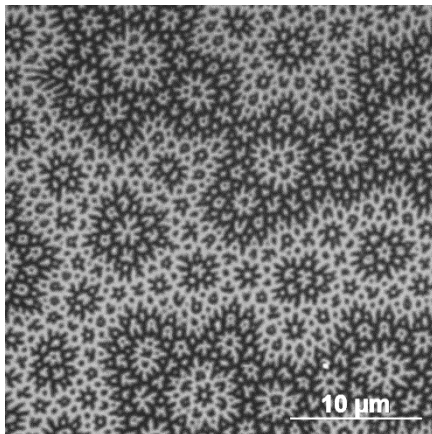
$\text{BaFe}_{12}\text{O}_{19}$ (hard ferrite)



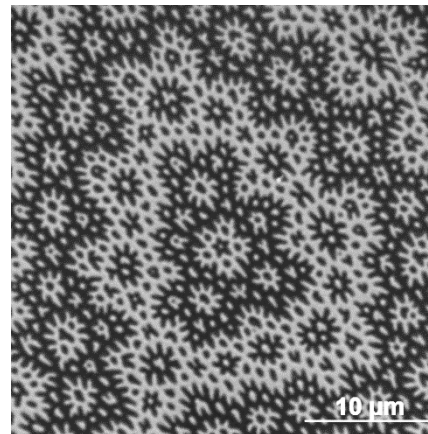
$\text{Ce}_2\text{Fe}_{14}\text{B}$



$\text{Y}_2\text{Fe}_{14}\text{B}$



$\text{Pr}_2\text{Fe}_{14}\text{B}$



$\text{Nd}_2\text{Fe}_{14}\text{B}$

| Literature values | J_s (T) |
|-------------------------------------|-----------|
| $\text{BaFe}_{12}\text{O}_{19}$ | ~0,3 |
| $\text{Ce}_2\text{Fe}_{14}\text{B}$ | 1,17 |
| $\text{Y}_2\text{Fe}_{14}\text{B}$ | 1,38 |
| $\text{Pr}_2\text{Fe}_{14}\text{B}$ | 1,56 |
| $\text{Nd}_2\text{Fe}_{14}\text{B}$ | 1,61 |